Oxapentadienyl−Rhodium−Phosphine Chemistry[1]

John R. Bleeke* and Edward Donnay

Department of Chemistry, Washington University, One Brookings Drive, St. Louis, Missouri 63130

Nigam P. Rath

Department of Chemistry, University of Missouri−St. Louis, 8001 Natural Bridge Road, St. Louis, Missouri 63121

Received March 31, 2002

Treatment of $[(PR_3)_2Rh(\mu\text{-Cl})]_2$ (R = Me or Et) with potassium oxapentadienide leads to the production of $((1-3-\eta)$-5-oxapentadienyl)$Rh(PR_3)_2$ (**1**, R = Me; **2**, R = Et) as equilibrium mixtures of anti and syn isomers. Similarly, treatment of $[(PR_3)_2Rh(\mu\text{-Cl})]_2$ (R = Me, Et) with potassium 2,4-dimethyloxapentadienide generates $((1-3-\eta)$-2,4-dimethyl-5-oxapentadienyl$)Rh(PR_3)_2$ (**3**, R = Me; **4**, R = Et). Compounds **3** and **4** exist predominantly as the anti isomer but upon cooling exhibit two rotameric forms, the sickle-shaped and U-shaped rotamers. Treatment of **1** with an additional 1 equiv of PMe_3 produces the 18e species $((1-3-\eta)$-5-oxapentadienyl$)Rh(PMe_3)_3$ (**5**), which is stable at room temperature. In contrast, when **2** is treated with an additional 1 equiv of PEt_3, no reaction can be detected by NMR at room temperature. However, upon cooling to −70 °C, the characteristic signals for the phosphine adduct $((1-3-\eta)$-5-oxapentadienyl$)Rh(PEt_3)_3$ (**6**) are observed by NMR. Compound **3**, like **1**, reacts with an additional 1 equiv of PMe_3 to produce $((1-3-\eta)$-2,4-dimethyl-5-oxapentadienyl$)$-$Rh(PMe_3)_3$ (**7**) at room temperature. Finally, treatment of **4** with PEt_3 yields no phosphine adduct, even upon cooling to −70 °C. Treatment of **4** with methyl triflate ($CH_3O_3SCF_3$) leads to methylation at the rhodium center and coordination of the oxapentadienyl C=O group, producing the 18e species $[(\eta^5$-2,4-dimethyl-5-oxapentadienyl$)Rh(PEt_3)_2(Me)]^+O_3SCF_3^-$ (**8**). Similarly, treatment of **4** with $HBF_4 \cdot OEt_2$ generates $[(\eta^5$-2,4-dimethyl-5-oxapentadienyl$)$-$Rh(PEt_3)_2(H)]^+BF_4^-$ (**9**), together with a novel isomer (**10**). Isomer **10** results from hydride migration to C3 of the 2,4-dimethyloxapentadienyl ligand, followed by metal-mediated activation of a methyl (C5) C−H bond. Treatment of **8** with PPN^+Cl^- results in chloride attack at the rhodium center and production of $((1-3-\eta)$-2,4-dimethyl-5-oxapentadienyl$)$-$Rh(PEt_3)_2(Me)(Cl)$ (**11**). In contrast, treatment of **9**/**10** with PPN^+Cl^- leads to hydride migration, dissociation of the resulting 2,4-dimethyloxapentadiene ligand, and production of $[(PEt_3)_2Rh(\mu\text{-Cl})]_2$. Compounds **1**, **5**, and **8** have been characterized by single-crystal X-ray diffraction.

Introduction

During the past two decades, the chemistry of metal complexes containing the acyclic pentadienyl group has been extensively investigated.[2] In contrast, relatively little effort has been directed toward synthesizing and studying the chemistry of (heteropentadienyl)metal complexes: i.e., species in which one of the terminal CH_2 groups of the pentadienyl ligand chain has been replaced with a heteroatom.[3] Like their pentadienyl analogues, these complexes promise to exhibit a variety of ligand bonding modes and a rich reaction chemistry based on facile ligand rearrangements.

In previous papers, we have described our systematic synthetic investigation of (heteropentadienyl)iridium complexes, using halo−iridium−phosphine compounds and anionic heteropentadienide reagents (including oxapentadienide,[4] thiapentadienide,[5] phosphapentadienide,[6] and azapentadienide[7] salts) as our building blocks. We now report our first synthetic foray into (heteropentadienyl)rhodium chemistry. As described herein, the reactions of $[(PR_3)_2Rh(\mu\text{-Cl})]_2$ precursors with anionic oxapentadienide and 2,4-dimethyloxapentadienide reagents have led to the production of four new (oxapentadienyl)$Rh(PR_3)_2$ complexes (**1**−**4**), and the reactivity of these electron-rich 16e complexes toward simple nucleophiles and electrophiles has been explored. X-ray crystal structures of representative complexes have been obtained, and a variety of interesting dynamic processes have been probed by variable-temperature NMR. To our knowledge, these are the first examples of (oxapentadienyl)rhodium complexes.

Results and Discussion

A. Synthesis, Structure, and Spectroscopy of (η^3-oxapentadienyl)$Rh(PR_3)_2$ Complexes. Treatment of

(1) Pentadienyl−Metal−Phosphine Chemistry. 31. Part 30: Bleeke, J. R.; Ortwerth, M. F.; Rohde, A. M. *Organometallics* **1995**, *14*, 2813.

(2) For reviews, see: (a) Ernst, R. D. *Chem. Rev.* **1988**, *88*, 1255. (b) Yasuda, H.; Nakamura, A. *J. Organomet. Chem.* **1985**, *285*, 15. (c) Powell, P. *Adv. Organomet. Chem.* **1986**, *26*, 125. (d) Ernst, R. D. *Comments Inorg. Chem.* **1982**, *21*, 285.

10.1021/om020429u CCC: $22.00
Publication on Web 08/24/2002

$[(PR_3)_2Rh(\mu\text{-}Cl)]_2$ (R = Me, Et)[8] with 2 equiv of potassium oxapentadienide[9] in tetrahydrofuran (THF) at −30 °C leads to the formation of ((1−3-η)-5-oxapentadienyl)-$Rh(PR_3)_2$ (**1**, R = Me; **2**, R = Et), as shown in Scheme 1. In each case, anti and syn isomers are produced in an equilibrium mixture. Similarly, treatment of $[(PR_3)_2Rh(\mu\text{-}Cl)]_2$ (R = Me, Et) with 2 equiv of potassium 2,4-dimethyloxapentadienide[10] produces ((1−3-η)-2,4-dimethyl-5-oxapentadienyl)$Rh(PR_3)_2$ (**3**, R = Me; **4**, R = Et) as equilibrium mixtures with the anti isomers greatly favored (Scheme 1). At room temperature, the anti/syn isomerization process is slow on the NMR time scale but rapid on the laboratory time scale.

1. ((1−3-η)-5-oxapentadienyl)$Rh(PMe_3)_2$ (1).[11] The ^1H, ^{13}C, and ^{31}P NMR spectra of ((1−3-η)-5-oxapentadienyl)$Rh(PMe_3)_2$ (**1**) in benzene-d_6 solution show two sets of peaks in an approximate 3:2 ratio, corresponding to the anti and syn isomers. In the ^1H NMR spectrum, downfield signals are observed at δ 8.57 and 9.55 for the formyl (H4) protons of the anti and syn isomers, respectively. The other oxapentadienyl proton signals all lie in the allylic region of the spectrum (δ 2.68−5.25). The H3 signal for the anti isomer appears significantly downfield from the corresponding signal for the syn isomer (δ 4.54 vs 3.54). This downfield shift may reflect the fact that H3 is directed away from the Rh center (and its shielding influence) in the anti isomer but toward the shielding metal center in the syn isomer. In the $^{13}C\{^1H\}$ NMR spectrum of **1**, there are two downfield singlets at δ 179.2 and 194.3, assigned to the formyl carbons (C4's) of the anti and syn isomers, respectively. The other peaks appear in the allylic region (δ 50.3−109.4) and carbons C1 and C3 exhibit significant couplings to the ^{31}P nuclei that lie trans to them (J_{C-P} = 16.5−21.7 Hz).

Scheme 1

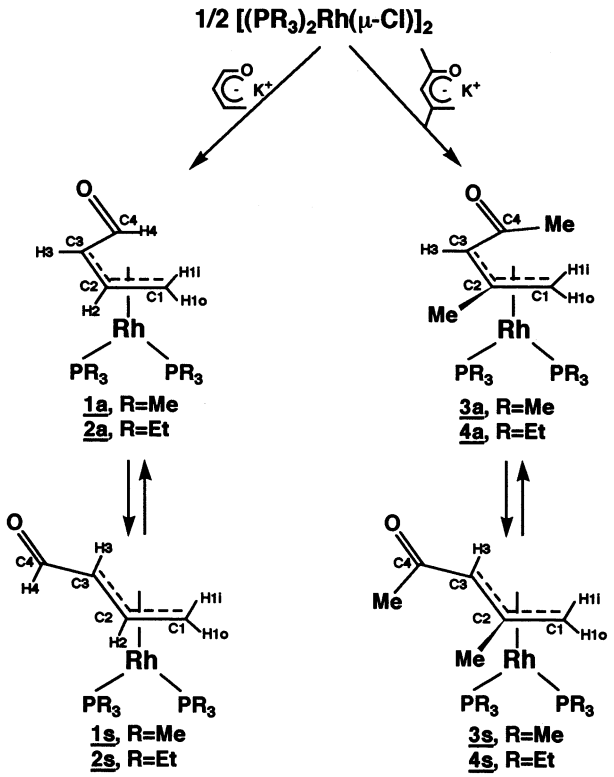

In the $^{31}P\{^1H\}$ NMR spectrum, *each* isomer gives rise to a pair of signals due to the inequivalent phosphine ligands. The signals are all doublet of doublets patterns, where the larger doublet splitting results from rhodium−phosphorus coupling (J_{Rh-P} = 181.5−193.6 Hz) and the smaller doublet splitting is due to phosphorus−phosphorus coupling (J_{P-P} = 37.5−42.3 Hz). The signals due to the major (anti) isomer are slightly broadened at room temperature, probably as a result of slow η^3-oxapentadienyl ligand rotation, which would exchange the environments of the two phosphine ligands. As the sample is cooled to 0 °C, the signals sharpen. The signals due to the minor (syn) isomer are sharp even at room temperature, reflecting a larger rotational barrier for the syn oxapentadienyl ligand.

The detailed solution-phase geometries of the two isomers were determined using 2D NOESY NMR spectroscopy. In the major isomer (**1a**), correlations between H2 and H3 and between $H1_i$ and H4 established the anti sickle-shaped geometry shown in Figure 1. Similarly, correlations between H2 and H4 and between $H1_i$ and H3 established the syn W-shaped geometry for the minor isomer (**1s**).

X-ray-quality crystals of **1** were obtained upon cooling a saturated diethyl ether solution of the equilibrium mixture to −30 °C. An ORTEP drawing is presented in Figure 2, and selected bond distances and angles are reported in the figure caption. The complex adopts a

(3) For examples of (oxapentadienyl)metal complexes, see: (a) Parshall, G. W.; Wilkinson, G. *Inorg. Chem.* **1962**, *1*, 896. (b) Tsuji, J.; Imamura, S.; Kiji, *J. Am. Chem. Soc.* **1964**, *86*, 4491. (c) Bannister, W. D.; Green, M.; Haszeldine, R. N. *J. Chem. Soc. A* **1966**, 194. (d) Green, M.; Hancock, R. I. *J. Chem. Soc. A* **1968**, 109. (e) Bennett, R. L.; Bruce, M. I. *Aust. J. Chem.* **1975**, *28*, 1141. (f) White, C.; Thompson, S. J.; Maitlis, P. M. *J. Organomet. Chem.* **1977**, *134*, 319. (g) Baudry, D.; Daran, J.-C.; Dromzee, Y.; Ephritikhine, M.; Felkin, H.; Jeannin, Y.; Zakrzewski, J. *J. Chem. Soc., Chem. Commun.* **1983**, 813. (h) Benyunes, S. A.; Green, M.; Grimshire, M. J. *Organometallics* **1989**, *8*, 2268. (i) Cheng, M.-H.; Wu, Y.-J.; Wang, S.-L.; Liu, R.-S. *J. Organomet. Chem.* **1989**, *373*, 119. (j) Cheng, M.-H.; Cheng, C.-Y.; Weng, S.-L.; Peng, S.-M.; Liu, R.-S. *Organometallics* **1990**, *9*, 1853. (k) Masters, A. P.; Richardson, J. F.; Sorensen, T. *Can. J. Chem.* **1990**, *68*, 2221. (l) Benyunes, S. A.; Day, J. P.; Green, M.; Al-Saadoon, A. W.; Waring, T. L. *Angew. Chem., Int. Ed. Engl.* **1990**, *29*, 1416. (m) Benyunes, S. A.; Binelli, A.; Green, M.; Grimshire, M. J. *J. Chem. Soc., Dalton Trans.* **1991**, 895. (n) Vong, W.-J.; Peng, S.-M.; Lin, S.-H.; Lin, W.-J.; Liu, R.-S. *J. Am. Chem. Soc.* **1991**, *113*, 573. (o) Schmidt, T.; Goddard, R. *J. Chem. Soc., Chem. Commun.* **1991**, 1427. (p) Trakarnpruk, W.; Arif, A. M.; Ernst, R. D. *Organometallics* **1992**, *11*, 1686. (q) Ogoshi, S.; Hirako, K.; Nakanishi, J.; Ohe, K.; Murai, S. *J. Organomet. Chem.* **1993**, *445*, C13. (r) AbuBaker, A.; Bryan, C. D.; Cordes, A. W.; Allison, N. T. *Organometallics* **1994**, *13*, 3375. (s) Pearson, A. J.; Neagu, I. B.; Pinkerton, A. A.; Kirschbaum, K.; Hardie, M. J. *Organometallics* **1997**, *16*, 4346. (t) Söderberg, B. C.; Berry, A.; Jones, P. C. *Organometallics* **1998**, *17*, 1069. (u) Beddows, C. J.; Box, M. R.; Butters, C.; Carr, N.; Green, M.; Kursawe, M.; Mahon, M. F. *J. Organomet. Chem.* **1998**, *550*, 267. (v) Navarro, M. E.; Chazaro, L. F.; Gonzalez, F. J.; Paz-Sandoval, M. A. *J. Electroanal. Chem.* **2000**, *480*, 18. (w) Clemente, M. E. N.; Saavedra, P. J.; Vasquez, M. C.; Paz-Sandoval, M. A.; Arif, A. M.; Ernst, R. D. *Organometallics* **2002**, *21*, 592.

(4) (a) Bleeke, J. R.; Haile, T.; Chiang, M. Y. *Organometallics* **1991**, *10*, 19. (b) Bleeke, J. R.; Haile, T.; New, P. R.; Chiang, M. Y. *Organometallics* **1993**, *12*, 517.

(5) (a) Bleeke, J. R.; Ortwerth, M. F.; Chiang, M. Y. *Organometallics* **1992**, *11*, 2740. (b) Bleeke, J. R.; Ortwerth, M. F.; Rohde, A. M. *Organometallics* **1995**, *14*, 2813.

(6) (a) Bleeke, J. R.; Rohde, A. M.; Robinson, K. *Organometallics* **1994**, *13*, 401. (b) Bleeke, J. R.; Rohde, A. M.; Robinson, K. D. *Organometallics* **1995**, *14*, 1674.

(7) Bleeke, J. R.; Luaders, S. T.; Robinson, K. D. *Organometallics* **1994**, *13*, 1592.

(8) Van der Ent, A.; Onderdelinden, O. *Inorg. Synth.* **1973**, *14*, 92.

(9) Heiszwolf, G. J.; Kloosterziel, H. *Recl. Trav. Chim. Pays-Bas* **1967**, *86*, 807.

(10) Bleeke, J. R.; Haile, T.; New, P. R.; Chiang, M. Y. *Organometallics* **1993**, *12*, 517.

(11) The simple η^3-allyl analogues of **1** and **5** have been reported: Sivak, A. J.; Muetterties, E. L. *J. Am. Chem. Soc.* **1979**, *101*, 4878.

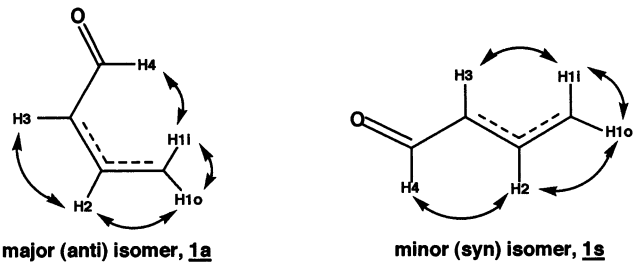

Figure 1. Significant correlations in the NOESY spectrum of ((1−3-η)-5-oxapentadienyl)Rh(PMe_3)$_2$ (**1**). The major isomer (**1a**) adopts the sickle-shaped anti geometry, while the minor isomer (**1s**) adopts the W-shaped syn geometry.

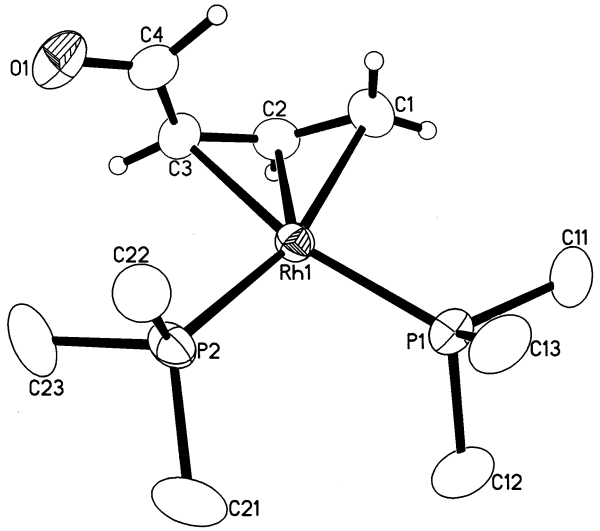

Figure 2. ORTEP drawing of ((1−3-η)-5-oxapentadienyl)-Rh(PMe_3)$_2$ (**1**), using thermal ellipsoids at the 50% probability level. Selected bond distances (Å): Rh−C1, 2.209(2); Rh−C2, 2.136(2); Rh−C3, 2.204(2); Rh−P1, 2.2523(6); Rh−P2, 2.2545(6); C1−C2, 1.390(3); C2−C3, 1.429(3); C3−C4, 1.436(3); C4−O1, 1.235(3). Note: the nonbonding Rh−C4 distance is 2.765 Å. Selected bond angles (deg): P1−Rh−P2, 97.61(2); C1−Rh−P1, 96.58(7); C3−Rh−P2, 97.59(7); C1−Rh−C3, 68.51(9); C1−Rh−P2, 162.57(7); C3−Rh−P1, 164.79(7); C1−C2−C3, 123.5(2); C2−C3−C4, 124.5(2); C3−C4−O1, 124.9(2).

distorted-square-planar coordination geometry with C1, C3, P1, and P2 occupying the four coordination sites. These four atoms and Rh are roughly coplanar with a mean deviation of 0.103Å. The oxapentadienyl ligand exhibits the η^3-anti sickle-shaped geometry, which is also the solution-phase geometry of the major isomer (vide supra). The torsional angle involving C2/C3/C4/O1 is 177.9°, close to the value of 180° for an idealized sickle shape. The torsional angle involving atoms C1/C2/C3/C4 is 24.3°, indicating that the formyl group is rotated out of the C1/C2/C3 plane away from the rhodium center. This rotation, which probably results from an unfavorable steric interaction between the formyl group and phosphine P2, causes C4 and O1 to lie 0.508 and 0.545 Å, respectively, out of the allyl plane. The bond distances within the allyl moiety are delocalized as expected (C1−C2 = 1.390(3) Å; C2−C3 = 1.429(3) Å). Interestingly, the bonds within the formyl group are also somewhat delocalized with C3−C4 (formally a single bond) exhibiting a relatively short bond distance of 1.436(3) Å and C4−O1 (formally a double bond) exhibiting a relatively long distance of 1.235(3) Å. These distances suggest that a second resonance structure (see **B**) may contribute to the overall bonding picture in **1**.

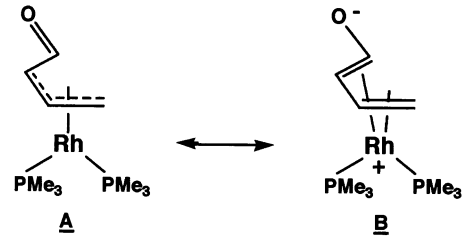

In this zwitterionic structure, the metal is coordinated to the oxapentadienyl ligand in an η^4 fashion. Also consistent with this picture is the relatively low energy C=O stretch in the IR spectrum (1589 cm^{-1}).

When crystals of **1a** are redissolved in benzene-d_6 at room temperature, they rapidly isomerize back to the equilibrium mixture of **1a** and **1s**.[12]

2. ((1−3-η)-5-oxapentadienyl)Rh(PEt_3)$_2$ (2). The spectroscopic features of ((1−3-η)-5-oxapentadienyl)Rh-(PEt_3)$_2$ (**2**) are virtually identical with those of **1** described above (see Experimental Section). Compound **2** exists in benzene solution as an equilibrium mixture of anti and syn isomers in a ratio of approximately 3:2. 2D NOESY experiments show that these ligands are sickle-shaped (anti) and W-shaped (syn) in solution. The NMR signals for the phosphine ligands in the anti isomer are broadened at room temperature, indicating slow rotation of the η^3-oxapentadienyl ligand with respect to the Rh(PEt_3)$_2$ moiety. These signals sharpen upon cooling to 0 °C. The NMR signals for the phosphines of the syn isomer are sharp, even at room temperature.

3. ((1−3-η)-2,4-dimethyl-5-oxapentadienyl)Rh-(PMe_3)$_2$ (3).[13] The NMR spectra for ((1−3-η)-2,4-dimethyl-5-oxapentadienyl)Rh(PMe_3)$_2$ again show the presence of two isomers in equilibrium, but in this case one isomer is strongly preferred; the ratio is approximately 11.5:1. From the position of the ^{1}H NMR signals for H3 (δ 4.21 in the major isomer vs δ 3.25 in the minor), it appears that the predominant species is the anti isomer. This has been confirmed by 2D NOESY experiments, which show a strong correlation between H3 and methyl group C5 (see Figure 3). Methyl group C6 correlates with $H1_i$ but also with H3, suggesting solution-phase rotation about the bond C3−C4 at room temperature. This idea is supported by variable-temperature NMR studies (vide infra). The minor species is almost certainly the syn isomer, but its signals are too weak to yield reliable NOESY cross-peaks. Therefore, the detailed ligand geometry is not known.

In the $^{31}P\{^1H\}$ NMR spectrum at room temperature, we observe pairs of signals for the two isomers and each signal is a doublet of doublets pattern due to ^{103}Rh coupling (J_{P-Rh} = 183.3−192.0 Hz) and ^{31}P coupling (J_{P-P} = 36.7−37.5 Hz). However, as the sample is cooled, the signals due to the major (anti) isomer broaden and, in fact, broaden at different rates. The

(12) This isomerization probably proceeds through a 14e C3-bound η^1-oxapentadienyl−rhodium intermediate in which C2−C3 bond rotation is facile.

(13) η^3-2,4-Dimethylpentadienyl analogues of **3** and **4** have been reported: Bleeke, J. R.; Donaldson, A. J. *Organometallics* **1986**, *5*, 2401.

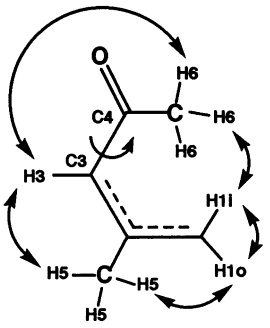

major (anti) isomer, 3a

Figure 3. Significant correlations in the NOESY spectrum of *anti*-((1−3-η)-2,4-dimethyl-5-oxapentadienyl)Rh(PMe_3)$_2$ (**3a**). The principal ligand geometry is the sickle-shaped structure shown, but a weak correlation between H3 and methyl C6 indicates rotation about the C3−C4 bond at room temperature.

signal at δ −12.1 broadens first, and then at lower temperature, the signal at δ −8.1 follows. Ultimately (at −70 °C), each signal resharpens into *two* new signals, indicating the presence of two new isomers in a 3:2 ratio.[14] We believe these species are the sickle- and U-shaped rotamers of the anti isomer:

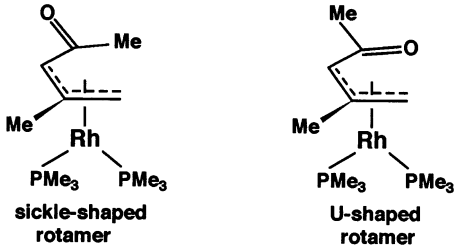

Throughout this temperature regime, the signals due to the minor (syn) isomer remain sharp.

Earlier, we noted that the X-ray structure of **1** suggests some delocalization and partial double-bond character between oxapentadienyl carbons C3 and C4 in the anti isomer. This partial double-bond character may also be present in the anti isomer of **3** and may explain why the two rotamers can be "frozen out" at low temperature. Interestingly, we do not observe rotamers upon cooling compound **1** to −90 °C. This suggests either that the rotation has not been arrested or that one rotamer (the sickle shape) dominates to the exclusion of the other.

4. ((1−3-η)-2,4-dimethyl-5-oxapentadienyl)Rh(PEt_3)$_2$ (4).[13] The NMR spectra for ((1−3-η)-2,4-dimethyl-5-oxapentadienyl)Rh(PEt_3)$_2$ (**4**) bear a striking resemblance to those of **3** (see Experimental Section). In this case, the anti isomer is even more dominant in the equilibrium mixture (>95%), and the peaks due to the syn isomer cannot be reliably assigned. Room-temperature 2D NOESY experiments show strong correlations between C5 methyl and H3 and between C6 methyl and $H1_i$, as expected for the sickle-shaped anti geometry. A weaker correlation is observed between C6 methyl and H3, suggesting that rotation about the bond C3−C4 can occur in solution at room temperature.

Scheme 2

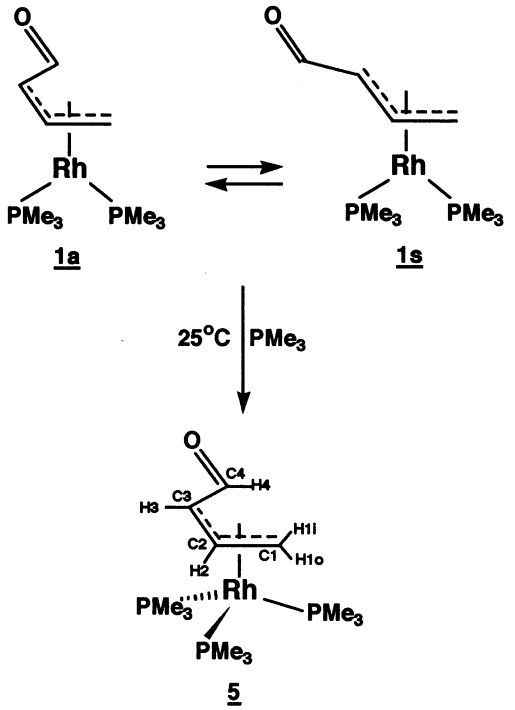

When compound **4** is cooled in toluene solution, the $^{31}P\{^1H\}$ NMR signals broaden and then resharpen into *two* pairs of doublet of doublets, indicating the presence of two isomers, probably sickle- and U-shaped rotamers of the anti isomer in an approximate 70:30 ratio. When compound **4** is warmed in toluene solution to 80 °C, the ^{31}P NMR peaks broaden, indicating that at this temperature, the η^3-2,4-dimethyloxapentadienyl ligand is spinning with respect to the Rh(PEt_3)$_2$ moiety.

B. Treatment of (η^3-oxapentadienyl)Rh(PR_3)$_2$ Complexes with PR_3. Synthesis, Structure, and Spectroscopy of (η^3-oxapentadienyl)Rh(PR_3)$_3$ Complexes. The (η^3-oxapentadienyl)Rh(PR_3)$_2$ complexes described above (compounds **1**−**4**) are coordinatively unsaturated 16e species. We therefore set out to investigate whether each of these species would add another phosphine ligand to generate the corresponding 18e tris(PR_3) complex. As described below, we found that these ligand addition reactions are very dependent on steric effects.

1. Addition of PMe_3 to ((1−3-η)-5-oxapentadienyl)Rh(PMe_3)$_2$ (1). As shown in Scheme 2, treatment of ((1−3-η)-5-oxapentadienyl)Rh(PMe_3)$_2$ (**1**) with 1 equiv of PMe_3 results in quantitative conversion to ((1−3-η)-5-oxapentadienyl)Rh(PMe_3)$_3$ (**5**).[11,15] The NMR spectra of this complex indicate that it is produced as a single isomer. The ^1H NMR spectrum features a single peak in the downfield region (δ 7.65), due to the formyl hydrogen, H4. Allylic protons H2 and H3 resonate at δ 4.72 and 4.25, respectively, while the allylic H1's appear at δ 1.25 and 1.07. The relatively downfield chemical shift position for H3 suggests that the oxapentadienyl ligand is anti, and this has been confirmed by 2D NOESY experiments, where a strong correlation between H2 and H3 is observed. A strong NOESY cross-

(14) At −70 °C, the two ^{31}P signals for the minor rotamer overlap coincidentally and hence appear as a single rhodium-coupled doublet.

(15) Compound **5** can also be synthesized by reacting (Cl)Rh(PMe_3)$_3$ with potassium oxapentadienide: see the Experimental Section.

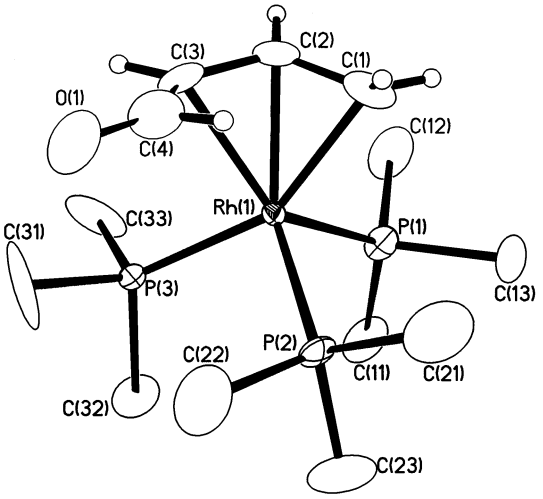

Figure 4. ORTEP drawing of ((1−3-η)-5-oxapentadienyl)-$Rh(PMe_3)_3$ (**5**), using thermal ellipsoids at the 25% probability level. Selected bond distances (Å): Rh−C1, 2.124(8); Rh−C2, 2.100(8); Rh−C3, 2.240(5); Rh−P1, 2.2665(10); Rh−P2, 2.295(2); Rh−P3, 2.318(2); C1−C2, 1.397(5); C2−C3, 1.413(5); C3−C4, 1.390(5); C4−O1, 1.189(8). Note: the nonbonding Rh−C4 distance is 2.795 Å. Selected bond angles (deg): P1−Rh−P2, 98.93(10); P1−Rh−P3, 100.61-(10); P2−Rh−P3, 99.45(4); C1−Rh−P3, 153.6(2); C2−Rh−P2, 133.5(3); C3−Rh−P1, 139.21(17); C1−Rh−C3, 66.5(2); C1−C2−C3, 117.0(8); C2−C3−C4, 130.9(7); C3−C4−O1, 139.3(13).

peak is also observed for $H1_i$ and H4, indicating a predominant sickle-shaped geometry. In the $^{13}C\{^1H\}$ NMR spectrum, C4 appears at δ 170.4 while C1, C2, and C3 resonate in the allylic region (δ 30.4−71.5). The C−P couplings observed for C1 and C3 in **5** (6.2 Hz) are significantly smaller than those observed for the same carbons in compound **1**.

Interestingly, the $^{31}P\{^1H\}$ spectrum for **5** at 25 °C consists of a single sharp doublet (J_{P-Rh} = 153.9 Hz), indicating rapid rotation of the η^3-oxapentadienyl ligand with respect to the $Rh(PMe_3)_3$ moiety.[16] As the sample is cooled to −70 °C, this signal gradually broadens and then reemerges as three separate phosphine resonances. Each of these new signals exhibits a substantial Rh−P coupling (J = 125.9−166.2 Hz) along with smaller P−P coupling. There is no evidence for separate sickle- and U-shaped rotamers at low temperature.

X-ray-quality crystals of **5** were obtained from a saturated diethyl ether solution at −30 °C. An ORTEP drawing is presented in Figure 4, while selected bond distances and angles are reported in the figure caption. The complex exhibits a "piano stool" structure with the three phosphine ligands serving as the legs and the η^3-oxapentadienyl ligand as the seat. In projection, phosphine P2 lies under the open allyl "mouth", while P1 and P3 lie roughly beneath the edges of the allyl moiety. As expected, the η^3-oxapentadienyl ligand is anti and sickle-shaped, consistent with the solution-phase geometry. The torsional angle C2/C3/C4/O1 is 179.6°, very close to the idealized value of 180° for a sickle shape.

(16) The equivalence of the three phosphine ligands *cannot* be explained by a rapid phosphine dissociation/reassociation process, because such a process would eliminate the Rh−P coupling. Furthermore, when compound **5** is treated with additional PMe_3, there is no broadening of the ^{31}P NMR signal for **5**, indicating that the PMe_3 ligands are not exchanging with free PMe_3 (on the NMR time scale).

Scheme 3

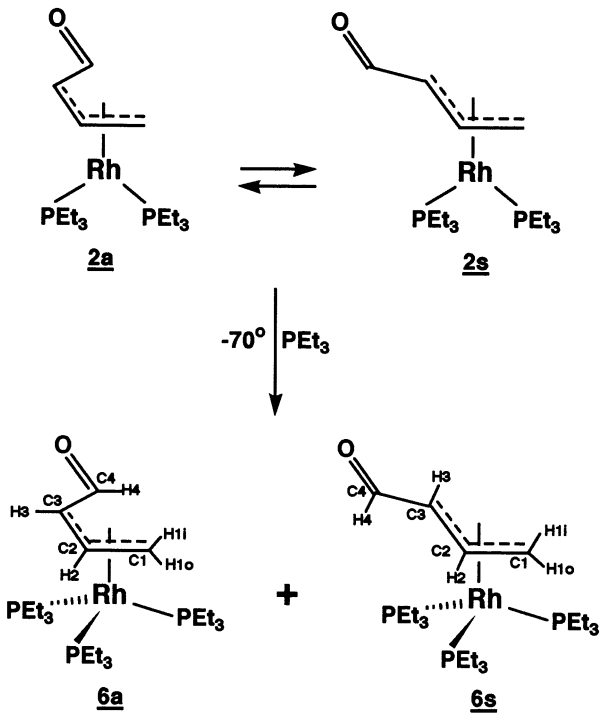

As in the structure of **1**, the formyl group is rotated out of the allyl plane. This rotation is reflected in a C1/C2/C3/C4 torsional angle of 18.0°, which causes atoms C4 and O1 to lie 0.326 and 0.375 Å, respectively, out of the C1/C2/C3 plane. The bonds within the allylic moiety of the oxapentadienyl ligand are delocalized, as expected, and the formyl group also appears to be somewhat delocalized, perhaps again reflecting a contribution by an (η^4-oxapentadienyl)Rh resonance structure.

2. Addition of PEt_3 to ((1−3-η)-5-oxapentadienyl)-$Rh(PEt_3)_2$ (2). When 1 equiv of PEt_3 is added to an NMR tube containing ((1−3-η)-5-oxapentadienyl)Rh-$(PEt_3)_2$ (**2**) in toluene-d_8 at room temperature, the ^1H NMR spectrum still shows the characteristic signals for **2**. There are no new signals corresponding to the production of a tris(phosphine) complex. However, the phosphine region of the ^1H NMR spectrum is now broad and the oxapentadienyl protons have lost their phosphorus coupling; they now exhibit only H−H coupling.

These ^1H NMR features are consistent with a rapid room-temperature phosphine exchange process involving coordinated (ligand) phosphines and free PEt_3. Most likely, this process involves PEt_3 attack on compound **2**, forming the 18e species (η^3-oxapentadienyl)$Rh(PEt_3)_3$ (**6**) as a transient intermediate. Rapid phosphine ligand loss from **6** then regenerates compound **2**. The $^{31}P\{^1H\}$ NMR spectrum is also consistent with this proposal. At room temperature, very broad humps are observed in the regions of the spectrum where compound **2** resonates (δ 15−35) and where free PEt_3 resonates (δ −15), indicating exchange of coordinated and free PEt_3.

However, as the sample is cooled, dramatic changes occur in both the ^1H and $^{31}P\{^1H\}$ NMR spectra. In the $^{31}P\{^1H\}$ NMR, the broad hump at δ 15−35 gradually sharpens until, at −70 °C, *two sets* of three signals are clearly discernible, indicating the presence of two tris-(phosphine) isomers (**6a** and **6s**) in a 2:1 ratio (see Scheme 3). The peaks due to the major isomer show

well-resolved Rh−P and P−P coupling, while those due to the minor isomer are less well resolved, suggesting that slow phosphine exchange is still occurring at −70 °C in the minor isomer. Similarly, in the ^{1}H NMR spectrum, the signals due to the two bis(phosphine) isomers (compound **2**) broaden as the sample is cooled.[17] Then two sets of new signals due to the two tris(phosphine) isomers (**6a** and **6s**) appear and begin to sharpen. At −70 °C, the H4, H3, and H2 signals for both isomers are well-resolved; the H1 signals are still broad and partially obscured by the phosphine signals.

From the chemical shift positions, it appears that the major isomer of **6** possesses the anti-η^3 ligand geometry. In particular, the H4 signal for the major isomer appears at δ 7.67, which correlates well with the position of H4 in the anti isomer of **5** (δ 7.65). In contrast, the signal for H4 in the minor isomer appears much farther downfield (δ 9.61), indicative of a syn geometry. Consistent with these isomer assignments are the chemical shift positions of the H3 protons. As expected, the H3 proton in the major (anti) isomer appears significantly downfield from that in the minor (syn) isomer (δ 4.74 vs 2.53).

It is interesting that both isomers of **6** (anti and syn) are observed at low temperature, while only the anti isomer of **5** is observed at room temperature and below. This may simply reflect the fact that **6** is formed by "trapping" the bis(phosphine) precursor **2** (which exists as anti and syn isomers) with PEt_3 at low temperature. The less stable syn isomer may not be able to isomerize to the more stable anti isomer under the low-temperature trapping conditions.

3. Addition of PMe_3 to ((1−3-η)-2,4-dimethyl-5-oxapentadienyl)Rh(PMe_3)$_2$ (3). The addition of 1 equiv of PMe_3 to ((1−3-η)-2,4-dimethyl-5-oxapentadienyl)Rh(PMe_3)$_2$ (**3**) in toluene-d_8 produces ((1−3-η)-2,4-dimethyl-5-oxapentadienyl)Rh(PMe_3)$_3$ (**7**) quantitatively.[18] This compound, like **5**, is observable by NMR at room temperature, but, unlike **5**, it exists as a mixture of anti and syn isomers in a ratio of approximately 4:1 (Scheme 4). In the ^{1}H NMR spectrum, the signal for H3 of the major isomer appears at δ 3.26, while that for the minor isomer is significantly upfield (δ 1.98). This strongly suggests that the major isomer possesses the anti ligand geometry, and this has been confirmed by 2D NOESY spectroscopy. In the NOESY spectrum, we see a strong correlation between H3 and the methyl group on C2 (methyl C5) in the major isomer. The ^{13}C{^{1}H} NMR spectrum of **7** shows the expected downfield peaks for C4 at δ 199.8 (anti) and δ 205.1 (syn). The allylic carbons are all in the normal allylic region (δ 38.2−86.9) and exhibit the expected couplings to phosphorus.

At room temperature, the ^{31}P{^{1}H} NMR spectrum of **7** is a broad hump with no discernible P−Rh coupling, reflecting a phosphine dissociation/reassociation process.[19,20] Upon cooling, the broad hump continues to broaden into the baseline and then reemerges at −20 °C as three well-separated humps. The humps ultimately sharpen at −50 °C into two overlapping sets of three peaks, corresponding to the two isomers of tris(phosphine) complex **7**. Each peak is a doublet of doublets of doublets pattern due to a large Rh−P coupling and two smaller P−P couplings.

Scheme 4

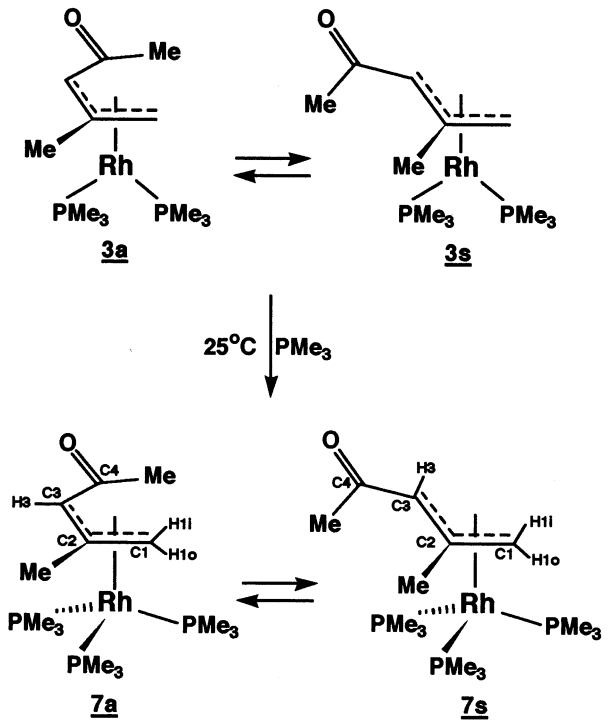

4. Addition of PEt_3 to ((1−3-η)-2,4-dimethyl-5-oxapentadienyl)Rh(PEt_3)$_2$ (4). When ((1−3-η)-2,4-dimethyl-5-oxapentadienyl)Rh(PEt_3)$_2$ (**4**) is treated with PEt_3, there is no reaction. The room-temperature ^{1}H NMR spectrum of this reaction mixture shows the characteristic peaks for **4** plus those for free PEt_3 with no apparent broadening (i.e., no exchange). Similarly, the ^{31}P{^{1}H} NMR spectrum exhibits the characteristic peaks for **4** plus a sharp singlet for free PEt_3. Furthermore, as the sample is cooled to −70 °C, no new peaks attributable to a tris(phosphine) product are observed.

C. Reactions of an (η^3-oxapentadienyl)Rh(PR_3)$_2$ Complex (4) with Electrophiles. Compounds **1**−**4** are electron-rich 16e complexes in which the oxapentadienyl C═O moiety remains uncoordinated to the rhodium center. We therefore became interested in the question of whether these complexes could be activated toward C═O coordination. We reasoned that removal of electron density from the metal center through formal oxidation should promote coordination of the C═O moiety. As a test of this idea, we treated ((1−3-η)-2,4-dimethyl-5-oxapentadienyl)Rh(PEt_3)$_2$ (**4**) with several electrophilic reagents, including methyl triflate ($CH_3O_3SCF_3$) and tetrafluoroboric acid (HBF_4·OEt_2), and found that the resulting Rh(III) centers did, in fact, coordinate the CO moiety.

1. Reaction of 4 with Methyl Triflate. Synthesis, Structure, and Spectroscopy of [(η^5-2,4-dimethyl-5-oxapentadienyl)Rh(PEt_3)$_2$(Me)]$^+$$O_3SCF_3^-$ (8).[21]

(17) A somewhat lower temperature is required to broaden the signals due to **2s** as compared to those due to **2a**.

(18) A slight excess of PMe_3 is added to **3** to ensure complete conversion to **7**: see Experimental Section.

(19) A small quantity of free PMe_3 is already in the NMR tube with **7** as a consequence of the synthesis procedure.[18] This free PMe_3 is thought to exchange with the coordinated (ligand) PMe_3's at room temperature.

(20) Phosphine dissociation is also indicated by the instability of **7** under vacuum, which has prevented its isolation.

Scheme 5

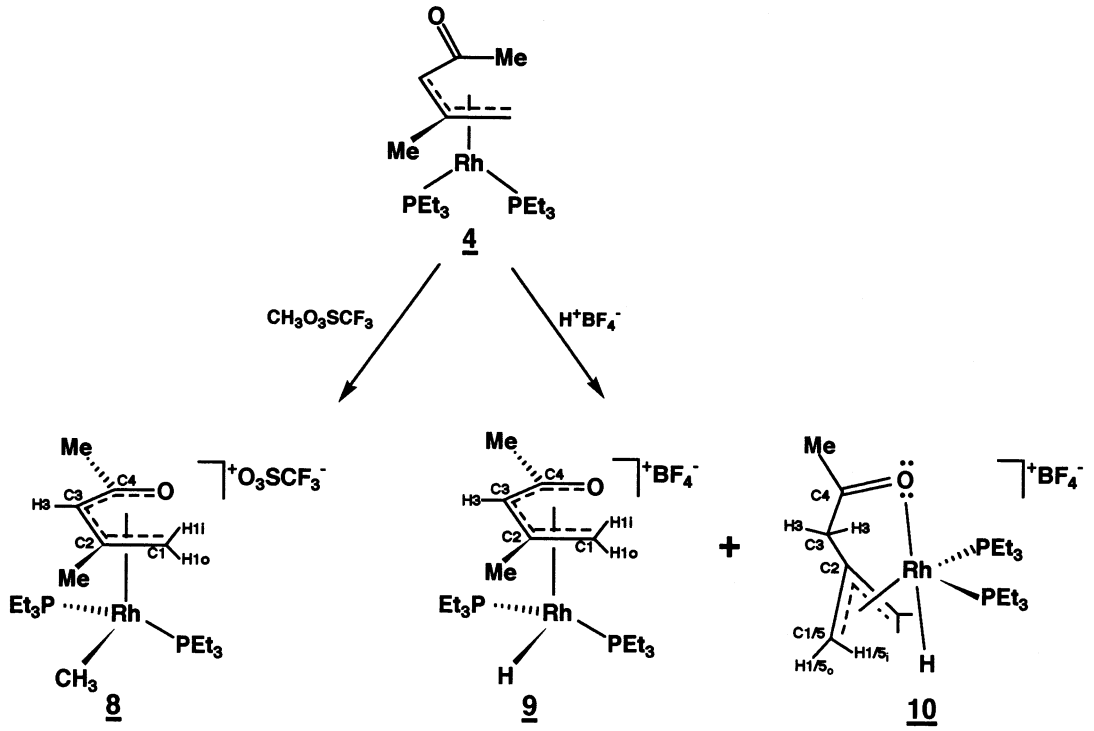

Treatment of ((1−3-η)-2,4-dimethyl-5-oxapentadienyl)-$Rh(PEt_3)_2$ (**4**) with methyl triflate ($CH_3O_3SCF_3$) in diethyl ether leads to methylation at the Rh(I) center and coordination of the C═O moiety, producing the 18e species [(η^5-2,4-dimethyl-5-oxapentadienyl)$Rh(PEt_3)_2$-(Me)]$^+O_3SCF_3^-$ (**8**) (see Scheme 5). In the ^{1}H NMR spectrum of **8**, the rhodium-bound methyl is observed as a multiplet at δ −0.05, while the oxapentadienyl protons resonate at δ 5.31 (H3), 3.24 ($H1_o$), and 2.95 ($H1_i$). The 2D NOESY spectrum shows a strong correlation between H3 and *both* oxapentadienyl methyl groups (C5 and C6), confirming the U-shaped geometry of the ligand. In the $^{13}C\{^1H\}$ NMR spectrum, the rhodium-based methyl resonates at δ −6.2 and appears as a doublet (J_{C-Rh} = 24.4 Hz) of triplets (J_{C-P} = 7.7 Hz). All of the oxapentadienyl carbons (C1→C4) are shifted downfield from their positions in **4**, as might be predicted, given the cationic nature of **8**. Oxapentadienyl carbons C1 and C3 are strongly coupled to phosphorus (J_{C1-P} = 32.1 Hz, J_{C3-P} = 21.8 Hz), indicating that these carbons lie approximately trans to phosphorus in the pseudo-octahedral coordination geometry of **8**; oxygen, therefore, resides approximately trans to the methyl ligand, as shown in Scheme 5. In the $^{31}P\{^1H\}$ NMR spectrum of **8**, the phosphines each give rise to a sharp doublet of doublets in which the larger coupling is due to rhodium (J_{P-Rh} = 136.3−152.6 Hz) and the smaller coupling is due to phosphorus (J_{P-P} = 20.5 Hz). The P−Rh coupling constants in **8** are reduced compared to those in precursor **4**, as is typical for a Rh(III) species.

Crystals suitable for X-ray diffraction were obtained by cooling a saturated diethyl ether solution of **8** to −30 °C. An ORTEP drawing of the solid-state structure is presented in Figure 5, while key bond distances and angles are reported in the figure caption. As expected,

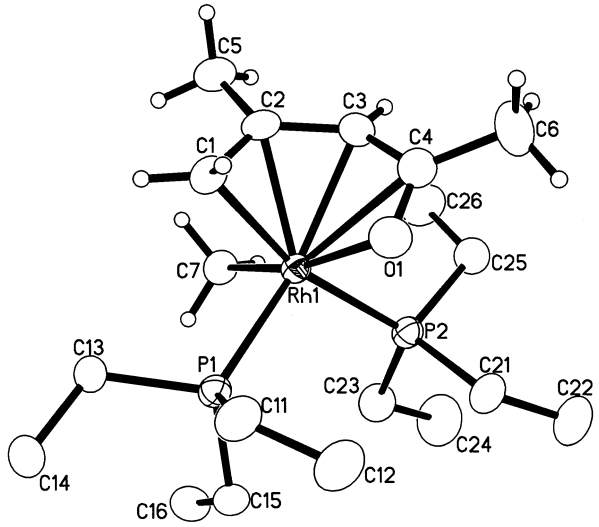

Figure 5. ORTEP drawing of the cation of [(η^5-2,4-dimethyl-5-oxapentadienyl)$Rh(PEt_3)_2(Me)]^+O_3SCF_3^-$ (**8**), using thermal ellipsoids at the 50% probability level. Selected bond distances (Å): Rh−C1, 2.198(3); Rh−C2, 2.226(3); Rh−C3, 2.284(3); Rh−C4, 2.587(3); Rh−O1, 2.309(2); Rh−P1, 2.2828(7); Rh−P2, 2.3389(7); Rh−C7, 2.070(3); C1−C2, 1.406(5); C2−C3, 1.421(4); C3−C4, 1.457(4); C4−O1, 1.246-(4); C2−C5, 1.505(4); C4−C6, 1.497(4). Selected bond angles (deg): P1−Rh−P2, 102.52(3); P1−Rh−C7, 89.30-(9); P2−Rh−C7, 90.71(9); C1−Rh−P2, 165.10(9); C3−Rh−P1, 152.81(8); O1−Rh−C7, 168.45(10); C1−C2−C3, 122.0-(3); C2−C3−C4, 123.4(3); C3−C4−O1, 119.7(3).

the molecule possesses a pseudo-octahedral coordination geometry with C1, C3, O1, P1, P2, and C7 occupying the six coordination sites; oxapentadienyl carbons C1 and C3 lie trans to phosphines, while O1 resides trans to methyl carbon C7. This arrangement places a large PEt_3 ligand (P1) under the open "mouth" of the η^5-oxapentadienyl ligand. Oxapentadienyl atoms C1, C2,

(21) 2,4-Dimethylpentadienyl analogues of **8** and **11** have been reported: Bleeke, J. R.; Donaldson, A. J. *Organometallics* **1988**, *7*, 1588.

C3, and O1 are essentially coplanar (mean deviation 0.005 Å), while C4 resides out of this plane (and away from Rh) by 0.34 Å. As a result, the Rh−C4 distance (2.587(3) Å) is substantially longer than the distance from Rh to the other four bound oxapentadienyl atoms (2.198−2.309 Å). This ligand nonplanarity suggests that the η^3:η^1 resonance structure **D** is a contributor (along

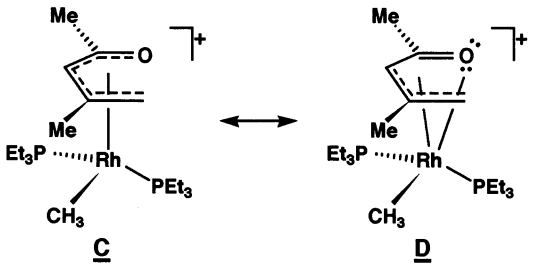

with the η^5 structure **C**) to the overall bonding picture in **8**. The bond distances within the oxapentadienyl ligand also seem to support this view. While the C1−C2 and C2−C3 distances (1.406(5) and 1.421(4) Å) are in the typical range for delocalized allyl or pentadienyl C−C bonds, the C3−C4 bond is significantly longer (1.457(4) Å), although clearly not long enough to be a true single bond. Similarly the C−O bond (1.246(4) Å) is shorter than a typical delocalized C−O bond but not short enough to be a true double bond.

2. Reaction of 4 with Tetrafluroboric Acid. Synthesis and Spectroscopy of [(η^5-2,4-dimethyl-5-oxapentadienyl)Rh(PEt_3)$_2$(H)]$^+BF_4^-$ (9) and Isomer 10. As shown in Scheme 5, treatment of ((1−3-η)-2,4-dimethyl-5-oxapentadienyl)Rh(PEt_3)$_2$ (**4**) with tetrafluroboric acid (HBF_4·OEt_2) in diethyl ether[22] leads to the synthesis of two isomeric products, [(η^5-2,4-dimethyl-5-oxapentadienyl)Rh(PEt_3)$_2$(H)]$^+BF_4^-$ (**9**) and a novel rearrangement product (**10**) in an approximate 3:1 ratio. The ^{1}H NMR spectrum of **9** features a metal−hydride signal at δ −24.53. The characteristic triplet of doublets pattern arises from coupling to the phosphine ligands (J_{H-P} = 24.9 Hz) and to the rhodium center (J_{H-Rh} = 17.4 Hz). The chemical shift positions of the oxapentadienyl protons in **9** are very similar to those in methyl analogue **8**; H3 resonates at δ 5.14, while the H1 signals are observed at δ 3.41 and 2.82. Similarly, the ^{13}C{^{1}H} NMR spectrum of **9** bears a close resemblance to that of **8**. Carbons C1 and C3 both exhibit substantial phosphorus coupling, indicating that they reside trans to the phosphines. The oxapentadienyl oxygen atom, therefore, lies trans to the hydride ligand in the pseudo-octahedral coordination geometry of **9**. Finally, the ^{31}P{^{1}H} NMR spectrum consists of two doublet of doublets signals, due to the two inequivalent phosphines. In each case, the large coupling is due to rhodium (J_{P-Rh} = 131.3 and 140.9 Hz), while the smaller coupling is due to the neighboring phosphine (J_{P-P} = 17.6 Hz).

The identity of the rearranged isomer, **10**, was established through a combination of NMR experiments. In the ^{1}H NMR spectrum, this compound also exhibited an upfield hydride signal (δ −24.84) which featured coupling to the phosphines and the rhodium center. However, in the ^{31}P{^{1}H} NMR spectrum, the compound exhibited only *one* signal, a rhodium-coupled doublet. These observations led us to conclude that the compound possessed mirror plane symmetry, which caused the phosphines to appear equivalent by NMR. Close inspection of the ^{1}H NMR spectrum showed the presence of only *one* methyl resonance, suggesting that the other methyl had undergone a C−H bond activation process. Furthermore, we found three equal-intensity resonances in the "allylic" region of the spectrum at δ 3.62, 3.47, and 2.76. These have since been assigned to $H1_o$/$H5_o$, H3's, and $H1_i$/$H5_i$, respectively (see labeling in Scheme 5). In the ^{13}C{^{1}H} NMR spectrum, equivalent allylic carbons C1 and C5 resonate at δ 56.1, while C3, an sp^3 carbon, appears upfield at δ 50.3. Ligand carbons C2 and C4 resonate at δ 126.6 and δ 227.1, respectively. C4's chemical shift position is significantly downfield from that observed in isomer **9** (δ 209.2), probably reflecting the fact that C4 is not coordinated to the Rh center in **10**.

While the identity of **10** has been confirmed by 2D HMQC and HMBC NMR experiments, the mechanism by which it is formed is not yet firmly established. Compound **9** and its isomer **10** do not interconvert, even upon heating in THF solution. This suggests that they are formed via separate, distinct pathways. One possibility, shown in Scheme 6, is that **9** and **10** result from different directions of H^+ attack. When H^+ attacks from below (i.e., opposite the acetyl group), the C=O moiety can coordinate immediately to stabilize the Rh(III) intermediate, generating compound **9** (path A). However, when the H^+ attacks from above (path B), coordination of the C=O moiety is blocked. In this case, the metal−hydride migrates to C3, producing a transient metal−olefin complex. This step is followed by activation of a C−H bond in methyl group C5 and coordination of the carbonyl oxygen to generate **10**.

D. Reactions of Electrophilic Addition Products 8 and 9/10 with Chloride. The electrophilic addition products, **8** and **9/10**, are 18e cationic species containing coordinated oxapentadienyl CO moieties. We were interested in whether these compounds would react with nuclophiles and, in particular, whether the reactions would result in displacement of the carbonyl groups from the rhodium centers. The chloride anion was selected as a representative nucleophilic reagent for this investigation.

1. Reaction of Compound 8 with PPN^+Cl^-. Synthesis and Spectroscopy of ((1−3-η)-2,4-dimethyl-5-oxapentadienyl)Rh(PEt_3)$_2$(Me)(Cl) (11).[21] Treatment of [((1−3-η)-2,4-dimethyl-5-oxapentadienyl)Rh(PEt_3)$_2$(Me)]$^+O_3SCF_3^-$ (**8**) with bis(triphenylphosphoranylidene)ammonium chloride (PPN^+Cl^-) in THF leads to chloride addition at the cationic Rh(III) center and decoordination of the C=O moiety, producing the 18e species ((1−3-η)-2,4-dimethyl-5-oxapentadienyl)Rh(PEt_3)$_2$(Me)(Cl) (**11**) (see Scheme 7). The uncoordinated CO bond is indicated by a strong absorption at 1658.6 cm^{-1} in the infrared spectrum. The ^{1}H NMR spectrum of **11** shows the presence of a single isomer with oxapentadienyl signals at δ 4.53 (H3), 3.81 ($H1_i$), and 3.28 ($H1_o$) and the rhodium−methyl signal at δ −0.03. The H3 signal is a phosphorus-coupled doublet (J_{H-P} = 7.8 Hz),

(22) The choice of solvent is important in this reaction. If arene solvents such as benzene or toluene are used, [(η^6-arene)Rh(PEt_3)$_2$]$^+$-BF_4^- products are formed, along with displaced 2,4-dimethyloxapentadiene. See ref 21 for a similar result in the analogous 2,4-dimethylpentadienyl system.

Scheme 6

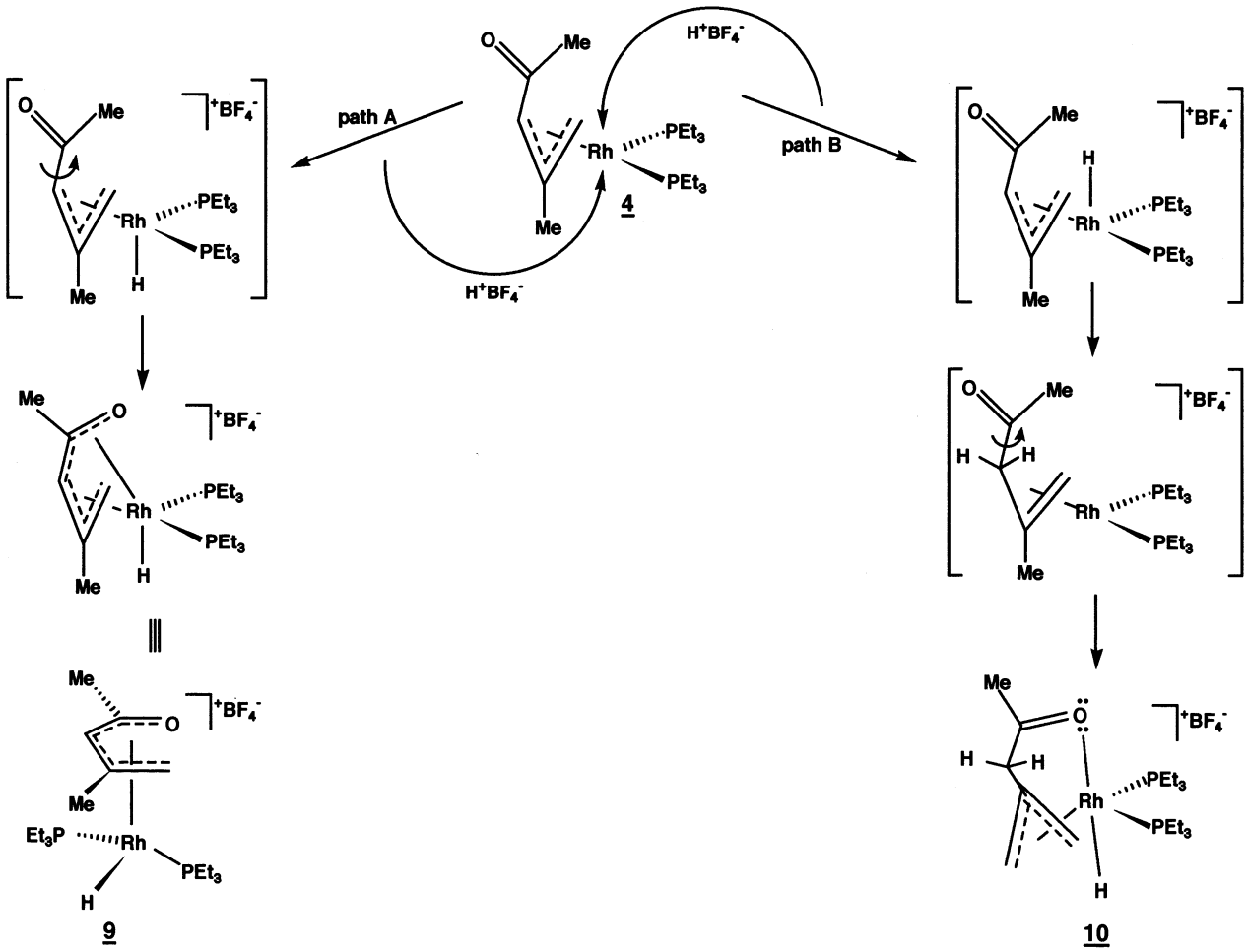

strongly suggesting a syn geometry for the η^3-oxapentadienyl ligand. This geometry has been confirmed by 2D NOESY spectroscopy, in which H3 correlates with $H1_i$[23] and with methyl C6 (the acetyl methyl) but not with methyl C5.

In the $^{13}C\{^1H\}$ NMR spectrum of **11**, C1 and C3 resonate at δ 62.3 and 72.1, respectively, and both are strongly coupled to phosphorus ($J_{C-P} = 30.4$ Hz in each case), indicating that these carbon atoms lie trans to the phosphines in the pseudo-octahedral coordination geometry of **11**. This leaves the methyl and chloro ligands to reside mutually trans to one another, as pictured in Scheme 7. The rhodium−methyl carbon resonates at δ −5.6 and is a doublet of triplets due to rhodium ($J_{C-Rh} = 21.9$ Hz) and phosphorus ($J_{C-P} = 6.9$ Hz) coupling.

The $^{31}P\{^1H\}$ NMR spectrum of **11** consists of two signals, consistent with the presence of two inequivalent phosphine ligands. Each signal is a doublet of doublets due to a large rhodium coupling and a smaller phosphorus coupling.

The formation of **11** probably involves an initial $\eta^5 \rightarrow \eta^3$ isomerization of the oxapentadienyl ligand, followed by Cl^- addition to the 16e cationic rhodium center. Subsequent $\eta^3 \rightarrow$ C3-η^1 oxapentadienyl isomerization, rotation, and reisomerization back to η^3 would produce the observed *syn*-η^3-oxapentadienyl product.

(23) Actually, H3 correlates with *both* H1's, suggesting that these protons are slowly exchanging, probably through the intermediacy of a C1-bound η^1-oxapentadienyl complex.

2. Reaction of Compounds 9/10 with PPN^+Cl^-. Formation of $[(PEt_3)_2Rh(\mu\text{-}Cl)]_2$. Treatment of the mixture of $[(\eta^5\text{-}2,4\text{-dimethyl-5-oxapentadienyl})Rh(PEt_3)_2(H)]^+BF_4^-$ (**9**) and isomer **10** with PPN^+Cl^- leads cleanly to the release of mesityl oxide (or its bond-migrated isomer) and formation of $[(PEt_3)_2Rh(\mu\text{-}Cl)]_2$. The rhodium dimer was unequivocally identified by comparison of its ^1H and $^{31}P\{^1H\}$ NMR spectra to those of an authentic sample. The proposed mechanism for the formation of $[(PEt_3)_2Rh(\mu\text{-}Cl)]_2$ from **9** is shown in Scheme 8. As before, $\eta^5 \rightarrow \eta^3$ isomerization of the oxapentadienyl ligand generates a cationic 16e intermediate, which reacts with Cl^- at rhodium. However, in this case, the η^3-oxapentadienyl and hydride ligands are unstable with respect to migratory insertion. Hydride migrates to either C1 or C3 of the oxapentadienyl ligand, and the resulting oxapentadiene dissociates. This leaves the 14e species $(PEt_3)_2Rh(Cl)$, which then dimerizes to $[(PEt_3)_2Rh(\mu\text{-}Cl)]_2$.

Summary

We have synthesized the first examples of (oxapentadienyl)rhodium complexes by treating $[(PR_3)_2Rh(\mu\text{-}Cl)]_2$ (R = Me, Et) with anionic oxapentadienide and 2,4-dimethyloxapentadienide reagents. The resulting (oxapentadienyl)$Rh(PR_3)_2$ complexes (**1**−**4**) are 16e species in which the oxapentadienyl ligands are coordinated in an η^3-allyl fashion to the rhodium centers. Treatment of ((1−3-η)-5-oxapentadienyl)$Rh(PMe_3)_2$ (**1**) or ((1−3-η)-

Scheme 7

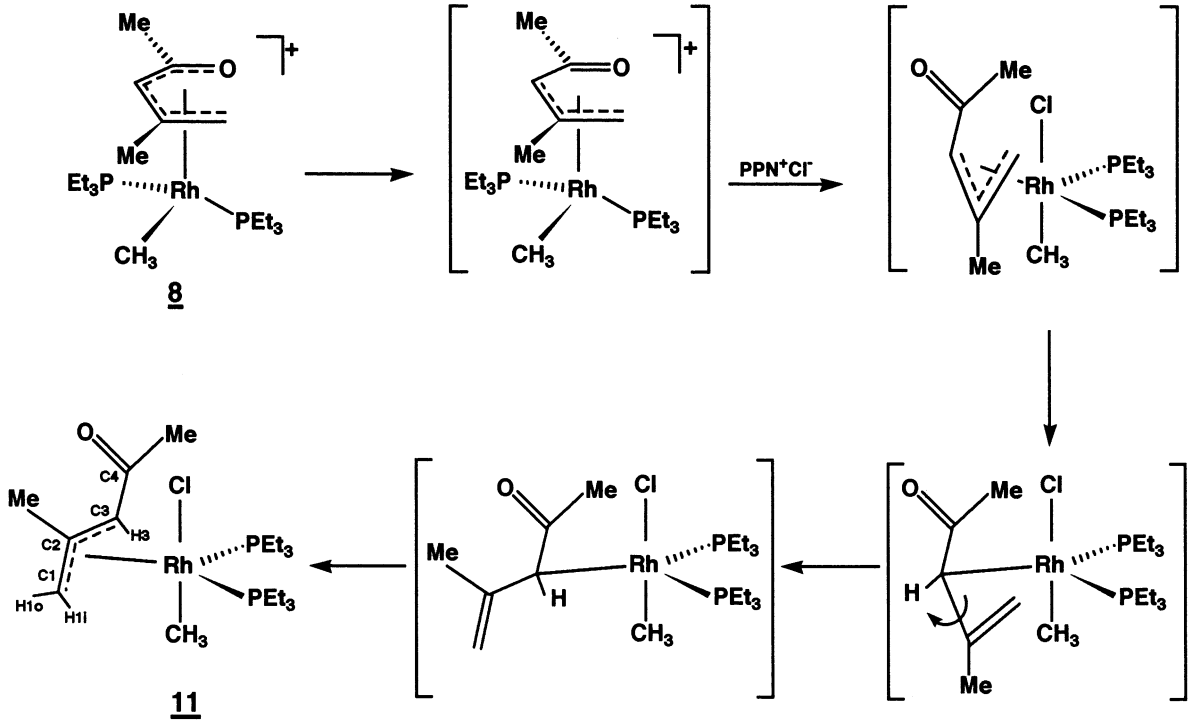

Scheme 8

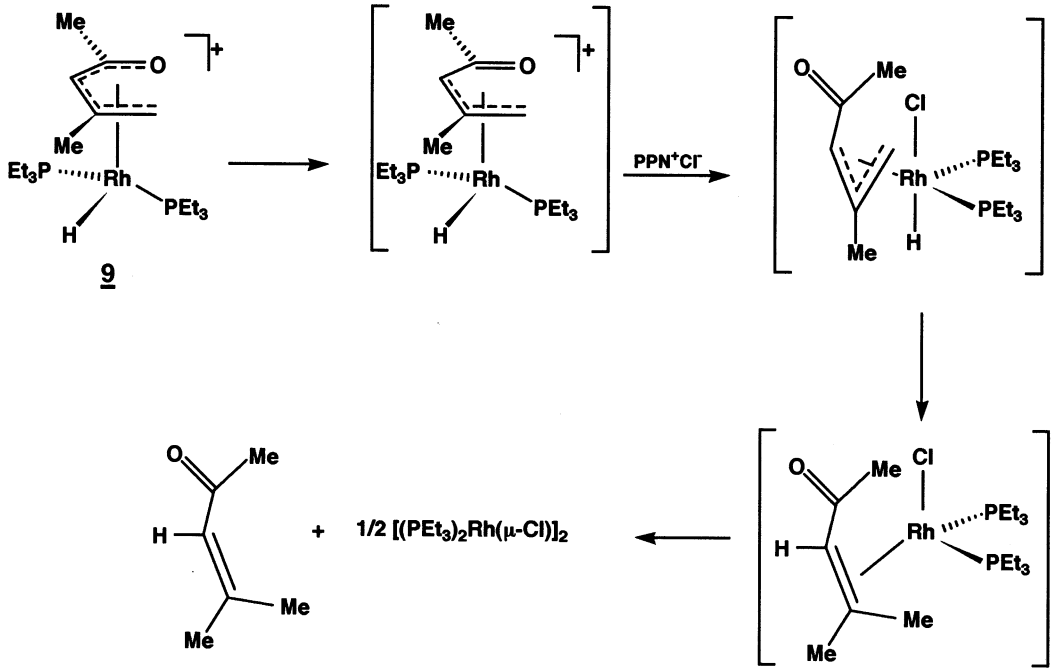

2,4-dimethyl-5-oxapentadienyl)Rh(PMe_3)$_2$ (**3**) with an additional 1 equiv of PMe_3 leads to the production of the corresponding 18e tris(PMe_3) complexes (**5** and **7**, respectively) at room temperature. In contrast, when ((1−3-η)-5-oxapentadienyl)Rh(PEt_3)$_2$ (**2**) is treated with additional PEt_3, the 18e adduct (**6**) is observed only at low temperature (by NMR), while ((1−3-η)-2,4-dimethyl-5-oxapentadienyl)Rh(PEt_3)$_2$ (**4**) is completely unreactive toward additional PEt_3. However, compound **4** does react with electrophiles such as methyl triflate or tetrafluoroboric acid to produce the 18e species [(η^5-2,4-dimethyl-5-oxapentadienyl)Rh(PEt_3)$_2$(Me)]$^+O_3SCF_3^-$ (**8**) and [(η^5-2,4-dimethyl-5-oxapentadienyl)Rh(PEt_3)$_2$(H)]$^+$-BF_4^- (**9**), respectively. These reactions involve electrophilic attack at the rhodium center, followed by coordination of the oxapentadienyl C=O moiety. Treatment of **8** with chloride leads to nucleophilic attack at rhodium and release of the C=O moiety, producing ((1−3-η)-2,4-dimethyl-5-oxapentadienyl)Rh(PEt_3)$_2$(Me)(Cl) (**11**). In contrast, treatment of **9** with Cl^- causes hydride migration, loss of the oxapentadiene ligand, and production of [(PEt_3)$_2$Rh(μ-Cl)]$_2$.

Experimental Section

General Comments. All manipulations were carried out under a nitrogen atmosphere, using either glovebox or double-

manifold Schlenk techniques. Solvents were stored under nitrogen after being distilled from the appropriate drying agents. Deuterated NMR solvents were obtained from Cambridge Isotope Laboratories or from Aldrich in sealed vials and used as received except for CD_2Cl_2, which was passed through neutral alumina to remove acid impurities. The following reagents were used as obtained from the supplier indicated: $RhCl_3 \cdot 3H_2O$ (Alfa Aesar), cyclooctene (Aldrich), trimethylphosphine (Strem), triethylphosphine (Strem), methyl triflate (Aldrich), tetrafluroboric acid−diethyl etherate (Aldrich), and bis(triphenylphosphoranylidene)ammonium chloride (PPN^+Cl^-; Aldrich).

The dimeric rhodium starting materials $[(PR_3)_2Rh(\mu\text{-}Cl)]_2$ (R = Me, Et), were prepared by adding 4 equiv of PR_3 to $[(C_8H_{14})_2Rh(\mu\text{-}Cl)]_2$[8] in THF. Similarly, $(Cl)Rh(PMe_3)_3$ was obtained by adding 6 equiv of PMe_3 to $[(C_8H_{14})_2Rh(\mu\text{-}Cl)]_2$. In each case, the phosphine addition was carried out at −30 °C, and the solution was stirred while slowly warming to room temperature. After filtration, the volatiles were removed under vacuum. Potassium oxapentadienide[9] and potassium 2,4-dimethyloxapentadienide[10] were prepared by literature procedures.

NMR experiments were performed on a Varian Unity Plus-300 spectrometer (^1H, 300 MHz; ^{13}C, 75 MHz; ^{31}P, 121 MHz), a Varian Mercury-300 spectrometer (^1H, 300 MHz; ^{13}C, 75 MHz; ^{31}P, 121 MHz), a Varian Unity Plus-500 spectrometer (^1H, 500 MHz; ^{13}C, 125 MHz; ^{31}P, 202 MHz), or a Varian Unity-600 spectrometer (^1H, 600 MHz; ^{13}C, 150 MHz; ^{31}P, 242 MHz). ^1H and ^{13}C spectra were referenced to tetramethylsilane, while ^{31}P spectra were referenced to external H_3PO_4. HMQC (^1H-detected multiple quantum coherence) and HMBC (heteronuclear multiple bond correlation) experiments aided in assigning some of the ^1H and ^{13}C peaks. 2D NOESY experiments provided spacial information, which allowed oxapentadienyl ligand shapes to be determined.

The infrared spectra were recorded on a Perkin-Elmer Spectrum BX FT-IR spectrometer.

Fast atom bombardment (FAB) mass spectra were obtained on a Kratos MS50 three-sector tandem mass spectrometer, while electron impact (EI) mass spectra were obtained on a VG ZAB-SE double-focusing instrument.

Microanalyses were performed by Galbraith Laboratories, Inc., Knoxville, TN.

Synthesis of ((1−3-η)-5-oxapentadienyl)Rh(PMe_3)$_2$ (1). $[(PMe_3)_2Rh(\mu\text{-}Cl)]_2$ (178 mg, 0.306 mmol) was dissolved in 15 mL of tetrahydrofuran (THF) and cooled to −30 °C. Similarly, potassium oxapentadienide (103 mg, 0.952 mmol) was also dissolved in THF (10 mL) and cooled to −30 °C. The oxapentadienide solution was added quickly to the cold rhodium starting material with stirring, and then the mixture was warmed to room temperature. The THF was removed under vacuum, and diethyl ether was added. The solution was then filtered through a glass frit, and the filtrate was dried in vacuo to give a dark orange solid. Cooling a saturated diethyl ether solution to −30 °C overnight produced suitable crystals for X-ray analysis. Yield of **1**: 135 mg (68%). The isomer ratio major (anti):minor (syn) was 3:2. Anal. Calcd for $C_{10}H_{23}OP_2Rh$: C, 37.05; H, 7.15. Found: C, 36.80; H, 7.35. FT-IR (Nujol): 1589.0 cm^{-1} (C═O stretch).

Major (anti) isomer: ^1H NMR (benzene-d_6, 25 °C) δ 8.57 (d, J_{H-H} = 8.4 Hz, 1, H4), 5.07 (m, 1, H2), 4.54 (m, 1, H3), 2.83 (br d, J_{H-H} = 7.2 Hz, 1, $H1_o$), 2.68 (br d, J_{H-H} = 13.2 Hz, 1, $H1_i$), 1.18 (br d, J_{H-P} = 7.8 Hz, 9, PMe_3), 1.01 (br d, H_{H-P} = 7.5 Hz, 9, PMe_3); $^{13}C\{^1H\}$ NMR (benzene-d_6, 25 °C) δ 179.2 (s, C4), 105.1 (d, J_{C-P} = 6.0 Hz, C2), 70.9 (dd, J_{C-P} = 16.5 Hz, 5.6 Hz, C3), 50.3 (dd, J_{C-P} = 19.3 Hz, 6.0 Hz, C1), 21.3 (br d, J_{C-P} = 25.4 Hz, PMe_3), 19.1 (br d, J_{C-P} = 22.9 Hz, PMe_3); $^{31}P\{^1H\}$ NMR (benzene-d_6, 25 °C) δ −10.1 (br dd, J_{P-Rh} = 193.6 Hz, J_{P-P} = 37.5 Hz, 1, PMe_3), −11.0 (br dd, J_{P-Rh} = 181.5 Hz, J_{P-P} = 37.5 Hz, 1, PMe_3).

Minor (syn) isomer: ^1H NMR (benzene-d_6, 25 °C) δ 9.55 (d, J_{H-H} = 8.4 Hz, 1, H4), 5.25 (m, 1, H2), 3.54 (m, 1, H3), 3.12 (m, 1, $H1_o$), 2.73 (dd, J = 13.8 Hz, 4.2 Hz, 1, $H1_i$), PMe_3's indistinguishable from those of the major isomer; $^{13}C\{^1H\}$ NMR (benzene-d_6, 25 °C) δ 194.3 (s, C4), 109.4 (d, J_{C-P} = 4.8 Hz, C2), 70.5 (dd, J_{C-P} = 18.1 Hz, 6.0 Hz, C3), 56.9 (dd, J_{C-P} = 21.7 Hz, 6.0 Hz, C1), 21.7 (d, J_{C-P} = 24.1 Hz, PMe_3), 18.6 (d, J_{C-P} = 25.4 Hz, PMe_3); $^{31}P\{^1H\}$ NMR (benzene-d_6, 25 °C) δ −6.3 (dd, J_{P-Rh} = 193.6 Hz, J_{P-P} = 42.3 Hz, 1, PMe_3), −12.0 (dd, J_{P-Rh} = 181.5 Hz, J_{P-P} = 42.3 Hz, 1, PMe_3).

Synthesis of ((1−3-η)-5-oxapentadienyl)Rh(PEt_3)$_2$ (2). $[(PEt_3)_2Rh(\mu\text{-}Cl)]_2$ (610 mg, 0.814 mmol) was dissolved in 25 mL of THF and cooled to −30 °C. Likewise, potassium oxapentadienide (301 mg, 2.782 mmol) was dissolved in THF (20 mL) and cooled to −30 °C. The oxapentadienide solution was added quickly to the cold rhodium starting material with stirring, and then this mixture was warmed to room temperature. The THF was removed under vacuum, and pentane was added. The solution was filtered through a glass frit and the filtrate was dried in vacuo to a red oil. Yield of **2**: 561 mg (84%). The isomer ratio major (anti):minor (syn) was 3:2.

The extreme air sensitivity of **2** rendered unsuccessful all attempts to obtain a high-resolution mass spectrum or an elemental analysis.

Major (anti) isomer: ^1H NMR (benzene-d_6, 25 °C) δ 8.55 (d, J_{H-H} = 9.0 Hz, 1, H4), 5.00 (m, 1, H2), 4.45 (m, 1, H3), 2.71 (d, J_{H-H} = 8.4 Hz, 1, $H1_o$), 2.56 (br d, J_{H-H} = 13.2 Hz, 1, $H1_i$), 1.74−1.47 (m, 12, PEt_3 CH_2's), 0.95−0.78 (m, 18, PEt_3 CH_3's); $^{13}C\{^1H\}$ NMR (benzene-d_6, 25 °C) δ 180.0 (s, C4), 103.0 (d, J_{C-P} = 6.9 Hz, C2), 69.9 (dd, J_{C-P} = 14.9 Hz, 5.7 Hz, C3), 49.2 (dd, J_{C-P} = 19.3 Hz, 6.7 Hz, C1), 21.1 (d, J_{C-P} = 20.8 Hz, PEt_3 CH_2's), 19.1 (d, J_{C-P} = 21.9 Hz, PEt_3 CH_2's), 8.9 (s, PEt_3 CH_3's); $^{31}P\{^1H\}$ NMR (benzene-d_6, 25 °C) δ 27.4 (br dd, J_{P-Rh} = 194.8 Hz, J_{P-P} = 33.4 Hz, 1, PEt_3), 22.5 (br dd, J_{P-Rh} = 182.6 Hz, J_{P-P} = 33.4 Hz, 1, PEt_3).

Minor (syn) isomer: ^1H NMR (benzene-d_6, 25 °C) δ 9.56 (d, J_{H-H} = 7.8 Hz, 1, H4), 5.16 (m, 1, H2), 3.42 (m, 1, H3), 3.04 (br s, 1, $H1_o$), 2.63 (dd, J = 13.2 Hz, 4.2 Hz, 1, $H1_i$), PEt_3 CH_2's and PEt_3 CH_3's indistinguishable from those of the major isomer; $^{13}C\{^1H\}$ NMR (benzene-d_6, 25 °C) δ 194.7 (s, C4), 107.4 (d, J_{C-P} = 5.1 Hz, C2), 69.7 (m, C3), 56.6 (dd, J_{C-P} = 20.5 Hz, 4.6 Hz, C1), 21.7 (d, J_{C-P} = 21.7 Hz, PEt_3 CH_2's), 18.0 (d, J_{C-P} = 21.9 Hz, PEt_3 CH_2's), 9.0 (s, PEt_3 CH_3's); $^{31}P\{^1H\}$ NMR (benzene-d_6, 25 °C) δ 32.4 (dd, J_{P-Rh} = 195.7 Hz, J_{P-P} = 37.5 Hz, 1, PEt_3), 23.8 (dd, J_{P-Rh} = 181.4 Hz, J_{P-P} = 37.5 Hz, 1, PEt_3).

Synthesis of ((1−3-η)-2,4-dimethyl-5-oxapentadienyl)-Rh(PMe_3)$_2$ (3). $[(PMe_3)_2Rh(\mu\text{-}Cl)]_2$ (168 mg, 0.289 mmol) was dissolved in 15 mL of THF and cooled to −30 °C. Potassium 2,4-dimethyloxapentadienide (121 mg, 0.867 mmol) was also dissolved in THF (10 mL) and cooled to −30 °C. The oxapentadienide solution was added quickly to the cold rhodium starting material with stirring, and then the mixture was warmed to room temperature. The THF was removed under vacuum, and pentane was added. The solution was filtered through a glass frit, and the filtrate was dried in vacuo to a yellow oil. Yield of **3**: 173 mg (85%). The isomer ratio major (anti):minor (syn) was 11.5:1. High-resolution EI-MS: calcd for $[M]^+$ ($C_{12}H_{27}RhOP_2^+$), 352.0592; found, 352.0589. FT-IR (Nujol): 1619.9 cm^{-1} (C═O stretch).

Major (anti) isomer: ^1H NMR (benzene-d_6, 25 °C) δ 4.21 (s, 1, H3), 3.60 (d, J_{H-P} = 6.6 Hz, 1, $H1_i$), 2.99 (s, 1, $H1_o$), 2.03 (s, 3, H6's), 1.72 (s, 3, H5's), 1.17 (d, J_{H-P} = 7.2 Hz, 9, PMe_3), 1.06 (d, J_{H-P} = 7.8 Hz 9, PMe_3); $^{13}C\{^1H\}$ NMR (benzene-d_6, 25 °C) δ 194.3 (s, C4), 116.0 (d, J_{C-P} = 6.0 Hz, C2), 71.4 (dd, J_{C-P} = 19.3 Hz, 7.2 Hz, C3), 56.1 (dd, J_{C-P} = 20.5 Hz, 6.0 Hz, C1), 30.5 (s, C6), 28.4 (s, C5), 22.0 (d, J_{C-P} = 24.1 Hz, PMe_3), 21.0 (d, J_{C-P} = 24.0 Hz, PMe_3); $^{31}P\{^1H\}$ NMR (benzene-d_6, 25 °C): δ −8.1 (dd, J_{P-Rh} = 188.8 Hz, J_{P-P} = 36.7 Hz, 1, PMe_3), −12.1 (dd, J_{P-Rh} = 184. 7 Hz, J_{P-P} = 36.7 Hz, 1, PMe_3).

At low temperature, two rotamers were observed for the anti isomer in an approximate 3:2 ratio.

Major rotamer: $^{31}P\{^1H\}$ NMR (toluene-d_8, −70 °C) δ −5.8 (dd, J_{P-Rh} = 187.3 Hz, J_{P-P} = 38.0 Hz, 1, PMe_3), −11.0 (dd, J_{P-Rh} = 186.1 Hz, J_{P-P} = 38.0 Hz, 1, PMe_3).

Minor rotamer: $^{31}P\{^1H\}$ NMR (toluene-d_8, −70 °C) δ −7.0 (d, J_{P-Rh} = 181.3 Hz, 2, PMe_3's).

Minor (syn) isomer: ^1H NMR (benzene-d_6, 25 °C) δ 3.25 (d, J_{H-P} = 6.0 Hz, 1, H3), 2.65 (m, 1, $H1_o$), 2.37 (s, 3, H5's), 2.35 (d, J_{H-P} = 6.6 Hz, 1, $H1_i$), 2.19 (s, 3, H6's), PMe_3 signals unidentifiable; $^{13}C\{^1H\}$ NMR (benzene-d_6, 25 °C) δ 204.1 (s, C4), 120.6 (s, C2), 65.1 (dm, J_{C-P} = 14.5 Hz, C3), 55.8 (dm, J_{C-P} = 22.1 Hz, C1), 32.6 (s, C6), 24.2 (s, C5), PMe_3 signals unidentifiable; $^{31}P\{^1H\}$ NMR (benzene-d_6, 25 °C) δ −5.8 (dd, J_{P-Rh} = 192.0 Hz, J_{P-P} = 37.5 Hz, 1, PMe_3), −16.5 (dd, J_{P-Rh} = 183.3 Hz, J_{P-P} = 37.5 Hz, 1, PMe_3).

Synthesis of ((1−3-η)-2,4-dimethyl-5-oxapentadienyl)Rh(PEt_3)$_2$ (4). $[(PEt_3)_2Rh(\mu\text{-}Cl)]_2$ (43 mg, 0.057 mmol) was dissolved in 4 mL of THF and cooled to −30 °C. Potassium 2,4-dimethyloxapentadienide (24 mg, 0.175 mmol) was also dissolved in THF (2 mL) and cooled to −30 °C. The oxapentadienide solution was added dropwise to the cold rhodium starting material with stirring, and then the mixture was warmed to room temperature. The THF was removed under vacuum, and pentane was added. The solution was filtered through a glass frit, and the filtrate was dried in vacuo to a red oil. Yield of **4**: 34 mg (68%). High-resolution EI-MS: calcd for $[M]^+$ ($C_{18}H_{39}RhOP_2^+$), 436.1531; found, 436.1546. FT-IR (Nujol): 1621.6 cm^{-1} (C═O stretch). ^1H NMR (benzene-d_6, 25 °C): δ 4.17 (br s, 1, H3), 3.35 (d, J_{H-P} = 6.0 Hz, 1, $H1_i$), 2.83 (s, 1, $H1_o$), 2.04 (s, 3, H6's), 1.74 (s, 3, H5's), 1.62−1.47 (m, 6, PEt_3 CH_2's), 1.41−1.33 (m, 6, PEt_3 CH_2's), 0.95−0.83 (m, 18, PEt_3 CH_3's). $^{13}C\{^1H\}$ NMR (benzene-d_6, 25 °C): δ 194.8 (s, C4), 114.2 (s, C2), 71.6 (d, J_{C-P} = 15.7 Hz, C3), 54.7 (d, J_{C-P} = 22.2 Hz, C1), 30.6 (s, C6), 28.1 (s, C5), 21.0 (d, J_{C-P} = 21.0 Hz, PEt_3 CH_2's), 20.0 (d, J_{C-P} = 20.9 Hz, PEt_3 CH_2's), 8.8 (s, PEt_3 CH_3's). $^{31}P\{^1H\}$ NMR (benzene-d_6, 25 °C): δ 30.7 (dd, J_{P-Rh} = 190.4 Hz, J_{P-P} = 33.6 Hz, 1, PEt_3), 25.2 (dd, J_{P-Rh} = 185.4 Hz, J_{P-P} = 33.6 Hz, 1, PEt_3).

At low temperature two rotamers were observed in an approximate 7:3 ratio.

Major rotamer: $^{31}P\{^1H\}$ NMR (toluene-d_8, −70 °C) δ 30.9 (dd, J_{P-Rh} = 188.4 Hz, J_{P-P} = 34.2 Hz, 1, PEt_3), 24.6 (dd, J_{P-Rh} = 180.4 Hz, J_{P-P} = 34.3 Hz, 1, PEt_3).

Minor rotamer: $^{31}P\{^1H\}$ NMR (toluene-d_8, −70 °C) δ 32.7 (dd, J_{P-Rh} = 189.2 Hz, J_{P-P} = 34.8 Hz, 1, PEt_3), 26.6 (dd, J_{P-Rh} = 190.5 Hz, J_{P-P} = 34.8 Hz, 1, PEt_3).

Synthesis of ((1−3-η)-5-oxapentadienyl)Rh(PMe_3)$_3$ (5). Method 1. (Cl)Rh(PMe_3)$_3$ (333 mg, 0.908 mmol) was dissolved in 10 mL of THF and cooled to −30 °C. Potassium oxapentadienide (147 mg, 1.359 mmol) was also dissolved in THF (5 mL) and cooled to −30 °C. The oxapentadienide solution was added quickly to the cold rhodium starting material with stirring, and then the mixture was warmed to room temperature. After 1 h, the THF was removed under vacuum. Multiple diethyl ether extractions were filtered through a glass frit, and the filtrate was dried in vacuo to a yellow-orange solid. Addition of a minimum amount of diethyl ether and cooling to −30 °C produced X-ray-quality crystals. Yield of **5**: 326 mg (90%).

Method 2. To a sample of ((1−3-η)-5-oxapentadienyl)Rh(PMe_3)$_2$ (**1**; 300 mg, 0.612 mmol) in 10 mL of THF was added PMe_3 (46.6 mg, 0.612 mmol) via syringe. The solution was stirred briefly, and the THF solvent was removed under vacuum. Multiple diethyl ether extractions were filtered through a glass frit, and the filtrate was dried in vacuo to a yellow-orange solid. Yield: 312 mg (90%).

Anal. Calcd for $C_{13}H_{32}OP_3Rh$: C, 39.01; H, 8.06. Found: C, 38.56; H, 8.08. FT-IR (Nujol): 1572.2 cm^{-1} (C═O stretch). ^1H NMR (benzene-d_6, 25 °C): δ 7.65 (d, J_{H-H} = 8.5 Hz, 1, H4), 4.72 (m, 1, H2), 4.25 (m, 1, H3), 1.25 (br s, 1, $H1_o$), 1.07 (br s, 1, $H1_i$), 1.01 (br s, 27, PMe_3's). $^{13}C\{^1H\}$ NMR (benzene-d_6, 25 °C): δ 170.4 (s, C4), 71.5 (d, J_{C-P} = 6.2 Hz, C3), 70.1 (d, J_{C-P} = 7.1 Hz, C2), 30.4 (br s, C1), 22.0 (br s, PMe_3's). $^{31}P\{^1H\}$ NMR (benzene-d_6, 25 °C): δ −16.1 (d, J_{P-Rh} = 153.9 Hz, PMe_3's). $^{31}P\{^1H\}$ NMR (toluene-d_8, −70 °C): δ −3.3 (dd, J_{P-Rh} = 166.2 Hz, J_{P-P} = 37.9 Hz, 1, PMe_3), −7.6 (br d, J_{P-Rh} = 125.9 Hz, 1, PMe_3), −25.0 (dd, J_{P-Rh} = 164.2 Hz, J_{P-P} = 37.9 Hz, 1, PMe_3).

Formation of ((1−3-η)-5-oxapentadienyl)Rh(PEt_3)$_3$ (6) at Low Temperature. To an NMR sample of ((1−3-η)-5-oxapentadienyl)Rh(PEt_3)$_2$ (**2**; 30 mg, 0.073 mmol) in toluene-d_8 was added PEt_3 (10 mg, 0.085 mmol) via syringe, and the mixture was shaken. Cooling to −70 °C allowed for spectroscopic identification of two isomers of **6**. The isomer ratio major (anti):minor (syn) was 2:1.

Major (anti) isomer: ^1H NMR (toluene-d_8, −70 °C) δ 7.67 (s, 1, H4), 4.93 (s, 1, H2), 4.74 (s, 1, H3), 2.0−0.05 (br m, 45, PEt_3 CH_2CH_3's), $H1_o$, $H1_i$ are obscured; $^{31}P\{^1H\}$ NMR (toluene-d_8, −70 °C) δ 21.5 (ddd, J_{P-Rh} = 164.1 Hz, J_{P-P} = 45.7 Hz, J_{P-P} = 18.8 Hz, 1, PEt_3), 13.4 (dd, J_{P-Rh} = 133.4 Hz, J_{P-P} = 18.8 Hz, 1, PEt_3), −1.0 (dd, J_{P-Rh} = 156.1 Hz, J_{P-P} = 45.7 Hz, 1, PEt_3).

Minor (syn) isomer: ^1H NMR (toluene-d_8, −70 °C) δ 9.61 (s, 1, H4), 5.61 (s, 1, H2), 2.53 (s, 1, H3), 2.0−0.5 (br m, 45, PEt_3 CH_2CH_3's), $H1_o$, $H1_i$ are obscured; $^{31}P\{^1H\}$ NMR (toluene-d_8, −70 °C) signals at δ 21.4, 16.5, and −2.3 are partially obscured by major isomer.

Synthesis of ((1−3-η)-2,4-dimethyl-5-oxapentadienyl)Rh(PMe_3)$_3$ (7). To an NMR sample of ((1−3-η)-2,4-dimethyl-5-oxapentadienyl)Rh(PMe_3)$_2$ (**3**; 39 mg, 0.111 mmol) in toluene-d_8, PMe_3 (11 mg, 0.145 mmol) was added via syringe and shaken. Compound **7** was fully characterized by NMR at 25 °C, but attempts to isolate it resulted in phosphine loss and slow decomposition. The isomer ratio major (anti):minor (syn) was 4:1.

Major (anti) isomer: ^1H NMR (toluene-d_8, 25 °C) δ 3.32 (s, 1, $H1_i$), 3.26 (s, 1, H3), 2.08 (s, 3, H5's), 1.99 (s, 3, H6's), 1.81 (s, 1, $H1_o$), 0.99 (s, 27, PMe_3's); $^{13}C\{^1H\}$ NMR (toluene-d_8, 25 °C) δ 199.8 s (C4), 86.9 (d, J_{C-P} = 7.0 Hz, C2), 59.8 (d, J_{C-P} = 7.9 Hz, C3), 39.5 (d, J_{C-P} = 8.9 Hz, C1), 31.4 (s, C6), 27.7 (s, C5), 21.4 (v br s, PMe_3's); $^{31}P\{^1H\}$ NMR (toluene-d_8, 25 °C) δ −14.0 (v br s, 3, PMe_3's); $^{31}P\{^1H\}$ NMR (toluene-d_8, −50 °C) δ 0.3 (ddd, J_{P-Rh} = 155.5 Hz, J_{P-P} = 27.8 Hz, 11.8 Hz, 1, PMe_3), −13.9 (ddd, J_{P-Rh} = 145.1 Hz, J_{P-P} = 58.4 Hz, J_{P-P} = 11.8 Hz, 1, PMe_3), −30.8 (dd, J_{P-Rh} = 148.2 Hz, J_{P-P} = 58.4 Hz, J_{P-P} = 27.8 Hz, 1, PMe_3).

Minor (syn) isomer: ^1H NMR (toluene-d_8, 25 °C) δ 2.61 (s, 3, H5's), 2.03 (s, 3, H6's), 1.98 (s, 1, H3), 1.48 (s, 1, $H1_o$), 0.83 (s, 1, $H1_i$), PMe_3's indistinguishable from major isomer; $^{13}C\{^1H\}$ NMR (toluene-d_8, 25 °C) δ 205.1 (s, C4), 82.5 (m, C2), 54.9 (m, C3), 38.2 (d, J_{C-P} = 9.8 Hz, C1), 32.3 (s, C6), 22.3 (s, C5), PMe_3's indistinguishable from major isomer; $^{31}P\{^1H\}$ NMR (toluene-d_8, 25 °C) indistinguishable from major isomer; $^{31}P\{^1H\}$ NMR (toluene-d_8, −50 °C) δ −0.2 (ddd, J_{P-Rh} = 161.9 Hz, J_{P-P} = 38.3 Hz, J_{P-P} = 22.4 Hz, 1, PMe_3), −29.9 (ddd, J_{P-Rh} = 142.9 Hz, J_{P-P} = 47.2 Hz, J_{P-P} = 38.3 Hz, 1, PMe_3), other PMe_3 obscured at ∼−14.

Synthesis of [(η^5-2,4-dimethyl-5-oxapentadienyl)Rh(PEt_3)$_2$(Me)]$^+$$O_3SCF_3^-$ (8). ((1−3-η)-2,4-dimethyl-5-oxapentadienyl)Rh(PEt_3)$_2$ (**4**; 435 mg, 0.997 mmol) was dissolved in 25 mL of diethyl ether and cooled to −30 °C. Using a syringe, 175 μL of methyl triflate (254 mg, 1.546 mmol) was added dropwise to the cold, stirred solution of **4**. An immediate reaction caused the solution's color to change from red to orange-yellow, and a solid formed. The precipitate was dried in vacuo to a red oily film, which was washed with pentane and diethyl ether to remove neutral impurities. The solid was then collected in acetone and dried. X-ray-quality crystals were obtained by dissolving the solid in a minimal quantity of THF, carefully layering diethyl ether on top for slow diffusion, and cooling to −30 °C. Yield of **8**: 558 mg (93%). Anal. Calcd for $C_{20}H_{42}F_3O_4P_2RhS$: C, 40.01; H, 7.05. Found: C, 39.84; H, 6.95.

Table 1. X-ray Diffraction Structure Summary

	1	5	8
formula	$C_{10}H_{23}OP_2Rh$	$C_{13}H_{32}OP_3Rh$	$C_{20}H_{42}F_3O_4P_2RhS$
fw	324.13	400.21	600.45
cryst syst	monoclinic	orthorhombic	orthorhombic
space group	$P2_1/n$	$Pna2_1$	$Pbca$
a, Å	9.5849(3)	19.1117(2)	16.4801(2)
b, Å	8.6359(2)	8.2583(1)	16.5822(2)
c, Å	17.5278(5)	12.0811(2)	19.6949(3)
α, deg	90.0	90.0	90.0
β, deg	95.600(2)	90.0	90.0
γ, deg	90.0	90.0	90.0
V, Å^3	1443.93(7)	1906.76(4)	5382.15(12)
Z	4	4	8
cryst dimens, mm	0.28 × 0.24 × 0.22	0.24 × 0.22 × 0.18	0.34 × 0.33 × 0.28
calcd density, g/cm^3	1.491	1.394	1.482
radiation; λ, Å	0.710 73	0.710 73	0.710 73
temp, K	190(2)	170(2)	180(2)
θ range, deg	2.33−28.36	2.69−29.00	2.03−30.02
data collected			
h	−12 to +12	−26 to +26	−23 to +23
k	−11 to +11	−11 to +11	−23 to +23
l	−23 to +23	−16 to +16	−27 to +27
total decay	none obsd	none obsd	none obsd
no. of data collected	35 603	48 874	145 645
no. of unique data	3603	5068	7737
Mo Kα linear abs coeff, mm^{-1}	1.377	1.137	0.874
abs cor applied	empirical (SADABS)	empirical (SADABS)	empirical (SADABS)
data to param ratio	16.45	31.09	25.96
final R indices (obsd data)[a]			
R1	0.0241	0.0402	0.0328
wR2	0.0540	0.0785	0.0679
R indices (all data)			
R1	0.0276	0.0475	0.0644
wR2	0.0551	0.0809	0.0886
goodness of fit	1.143	1.137	1.096

[a] $I > 2\sigma(I)$.

High-resolution FAB-MS: calcd for $[M]^+$ ($C_{19}H_{42}OP_2Rh$), 451.1766; found, 451.1757. FT-IR (Nujol): 1590.9 cm^{-1} (C═O stretch). ^{1}H NMR (CD_2Cl_2, 25 °C): δ 5.31 (br s, 1, H3), 3.24 (s, 1, H1$_o$), 2.95 (d, J_{H-P} = 8.4 Hz, 1, H1$_i$), 2.21 (s, 3, H6's), 2.13−1.99 (m, 6, PEt_3 CH_2's), 1.98−1.88 (m, 3, PEt_3 CH_2's), 1.90 (s, 3, H5's), 1.77−1.69 (m, 3, PEt_3 CH_2's), 1.24−1.18 (m, 9, PEt_3 CH_3's), 1.14−1.09 (m, 9, PEt_3 CH_3's), −0.05 (m, 3, Rh−CH_3); ^{13}C{^{1}H} NMR (CD_2Cl_2, 25 °C) δ 210.2 (d, J_{C-P} = 3.9 Hz, C4), 132.7 (s, C2), 76.2 (d, J_{C-P} = 21.8 Hz, C3), 56.6 (dd, J_{C-P} = 32.1 Hz, 6.4 Hz, C1), 31.2 (s, C6), 22.6 (s, C5), 19.5 (d, J_{C-P} = 28.2 Hz, PEt_3 CH_2's), 18.8 (d, J_{C-P} = 24.3 Hz, PEt_3 CH_2's), 8.1−7.7 (m, PEt_3 CH_3's), −6.2 (dt, J_{C-Rh} = 24.4 Hz, J_{C-P} = 7.7 Hz, 3, Rh−CH_3); ^{31}P{^{1}H} NMR (CD_2Cl_2, 25 °C) δ 27.3 (dd, J_{P-Rh} = 152.6 Hz, J_{P-P} = 20.5 Hz, 1, PEt_3), 12.4 (dd, J_{P-Rh} = 136.3 Hz, J_{P-P} = 20.5 Hz, 1, PEt_3).

Synthesis of [(η^5-2,4-dimethyl-5-oxapentadienyl)Rh(PEt$_3$)$_2$(H)]$^+$BF$_4^-$ (9) and Isomer 10. ((1−3-η)-2,4-dimethyl-5-oxapentadienyl)Rh(PEt_3)$_2$ (**4**; 506 mg, 1.160 mmol) was dissolved in 25 mL of diethyl ether and cooled to −30 °C. Using a syringe, 200 μL of tetrafluroboric acid−diethyl etherate (220 mg, 1.359 mmol) was added dropwise to the cold, stirred solution. An oily solid was formed, together with a red solution. Removal of the solvents under vacuum produced a red oily film, which was washed with pentane and diethyl ether to remove neutral impurities. The solid was then collected in methylene chloride and dried. Yield of **9** and **10**: 524 mg (86%). The major to minor isomer ratio is 3:1. High-resolution FAB-MS: calcd for $[M]^+$ ($C_{18}H_{40}OP_2Rh$) 437.1609, found 437.1596.

Major isomer (**9**): ^{1}H NMR (CD_2Cl_2, 25 °C) δ 5.14 (s, 1, H3), 3.41 (s, 1, H1$_o$), 2.82 (d, J_{H-P} = 8.4 Hz, 1, H1$_i$), 2.26 (s, 3, H6's), 2.05 (s, 3, H5's), 2.3−1.7 (m, 12, PEt_3 CH_2's), 1.4−1.0 (m, 18, PEt_3 CH_3's), −24.53 (td, J_{H-P} = 24.9 Hz, J_{H-Rh} = 17.4 Hz, 1, Rh−H); ^{13}C{^{1}H} NMR (CD_2Cl_2, 25 °C) δ 209.2 (s, C4), 129.8 (s, C2), 75.6 (d, J_{C-P} = 17.0 Hz, C3), 58.4 (dd, J_{C-P} = 27.5 Hz, 6.6 Hz, C1), 31.0 (s, C6), 25.4 (s, C5), 21.1 (d, J_{C-P} = 26.3 Hz, PEt_3 CH_2's), 20.4 (d, J_{C-P} = 30.2 Hz, PEt_3 CH_2's), 8.2−7.8 (m, PEt_3 CH_3's); ^{31}P{^{1}H} NMR (CD_2Cl_2, 25 °C) δ 39.6 (dd, J_{P-Rh} = 140.9 Hz, J_{P-P} = 17.6 Hz, 1, PEt_3), 25.7 (dd, J_{P-Rh} = 131.3 Hz, J_{P-P} = 17.6 Hz, 1, PEt_3).

Minor isomer (**10**): ^{1}H NMR (CD_2Cl_2, 25 °C) δ 3.62 (s, 2, H1$_o$/H5$_o$), 3.47 (s, 2, H3's), 2.76 (br d, J_{H-P} = 6.0 Hz, 2, H1$_i$/H5$_i$), 2.12 (s, 3, H6's), −24.84 (td, J_{H-P} = J_{H-Rh} = 17.4 Hz, 1, Rh−H), PEt_3 CH_2's and PEt_3 CH_3's are indistinguishable from major isomer; ^{13}C{^{1}H} NMR (CD_2Cl_2, 25 °C) δ 227.1 (s, C4), 126.6 (s, C2), 56.1 (m, C1/C5), 50.3 (s, C3), 29.6 (s, C6), PEt_3 CH_2's and PEt_3 CH_3's are indistinguishable from major isomer; ^{31}P{^{1}H} NMR (CD_2Cl_2, 25 °C) δ 28.7 (d, J_{P-Rh} = 137.0 Hz, PEt_3's).

Synthesis of ((1−3-η)-2,4-dimethyl-5-oxapentadienyl)-Rh(PEt$_3$)$_2$(Me)(Cl) (11). [(η^5-2,4-dimethyl-5-oxapentadienyl)-Rh(PEt_3)$_2$(Me)]$^+$O$_3$SCF$_3^-$ (**8**; 402 mg, 0.669 mmol) was dissolved in 50 mL of tetrahydrofuran and cooled to −30 °C. Solid bis(triphenylphosphoranylidene)ammonium chloride (PPN$^+$Cl$^-$; 425 mg, 0.740 mmol) was added to the cold, stirred solution of **8**. After addition of 20 mL of pentane the reaction mixture was filtered through a glass frit to remove unreacted PPN$^+$Cl$^-$. The solvent was removed to give a yellow-brown film. A diethyl ether extraction followed by filtration gave a yellow solution of the product, which was dried in vacuo to an oil. Yield of **11**: 189 mg (58%). FT-IR (Nujol): 1658.6 cm^{-1} (C═O stretch). ^{1}H NMR (benzene-d_6, 25 °C): δ 4.53 (d, J_{H-P} = 7.8 Hz, 1, H3), 3.81 (d, J_{H-P} = 7.8 Hz, 1, H1$_i$), 3.28 (br s, 1, H1$_o$), 2.21 (s, 3, H6's), 2.10 (s, 3, H5's), 1.88−1.60 (m, 12, PEt_3 CH_2's), 0.99−0.80 (m, 18, PEt_3 CH_3's), −0.03 (td, J_{H-P} = 4.8 Hz, J_{H-Rh} = 1.8 Hz, 3, Rh−CH_3). ^{13}C{^{1}H} NMR (benzene-d_6, 25 °C): δ 204.9 (s, C4), 131.5 (s, C2), 72.1 (dd, J_{C-P} = 30.4 Hz, 4.1 Hz, C3), 62.3 (dd, J_{C-P} = 30.4 Hz, 5.5 Hz, C1), 33.3 (s, C6), 19.6 (s, C5), 18.5 (d, J_{C-P} = 24.7 Hz, PEt_3 CH_2's), 18.2 (d, J_{C-P} = 23.4 Hz, PEt_3 CH_2's), 9.0 (d, J_{C-P} = 4.1 Hz, PEt_3 CH_3's), 8.4 (d, J_{C-P} = 4.1 Hz, PEt_3 CH_3's), −5.6 (dt, J_{C-Rh} = 21.9 Hz, J_{C-P} = 6.9 Hz, Rh−CH_3). ^{31}P{^{1}H} NMR (CD_2Cl_2, 25 °C): δ 22.4 (dd, J_{P-Rh} =

147.1 Hz, $J_{P-P} = 17.0$ Hz, 1, PEt_3), 10.2 (dd, $J_{P-Rh} = 137.9$ Hz, $J_{P-P} = 17.0$ Hz, 1, PEt_3).

X-ray Diffraction Studies of 1, 5, and 8. Single crystals of compounds **1**, **5**, and **8** were mounted on glass fibers under a nitrogen atmosphere. X-ray data were collected on a Bruker SMART charge coupled device (CCD) detector system at low temperature. Graphite-monochromated Mo Kα radiation was supplied by a sealed-tube X-ray source.

Structure solution and refinement were carried out using the SHELXTL-PLUS software package (PC version).[24] The rhodium atom positions were determined by direct methods. The remaining non-hydrogen atoms were found by successive full-matrix least-squares refinement and difference Fourier map calculations. In general, non-hydrogen atoms were refined anisotropically, while hydrogen atoms were placed at idealized positions and assumed the riding model.

Our assignment of the absolute configuration of compound **5** was based on a comparison of the Flack *x* parameter for the two enantiomorphs; the reported structure exhibited a lower value than the inverted structure.

(24) Sheldrick, G. M. SHELXTL-PLUS; Bruker Analytical X-ray Division, Madison, WI, 1997.

Crystal data and details of both collection and structure analysis are listed in Table 1.

Acknowledgment. Support from the National Science Foundation and the donors of the Petroleum Research Fund, administered by the American Chemical Society, is gratefully acknowledged. Washington University's High Resolution NMR Service Facility was funded in part by NIH Support Instrument Grants (Grant Nos. RR-02004, RR-05018, and RR-07155). Mass spectrometry was provided by the Washington University Mass Spectrometry Resource, an NIH Research Resource (Grant No. P41RR00954).

Supporting Information Available: Structure determination summaries and listings of final atomic coordinates, thermal parameters, bond lengths, and bond angles for compounds **1**, **5**, and **8.** This material is available free of charge via the Internet at http://pubs.acs.org.

OM020429U